

1 Q. **Reference: Assessment of Labrador Island Transmission Link (LIL) Reliability in Consideration**
2 **of Climatological Loads, March 10, 2021 (Haldar Report) by Dr. Asim Haldar, Ph.D., P. Eng.**
3 **page 13, lines 407-409**

4 Provide a copy of the 2009 Haldar study.

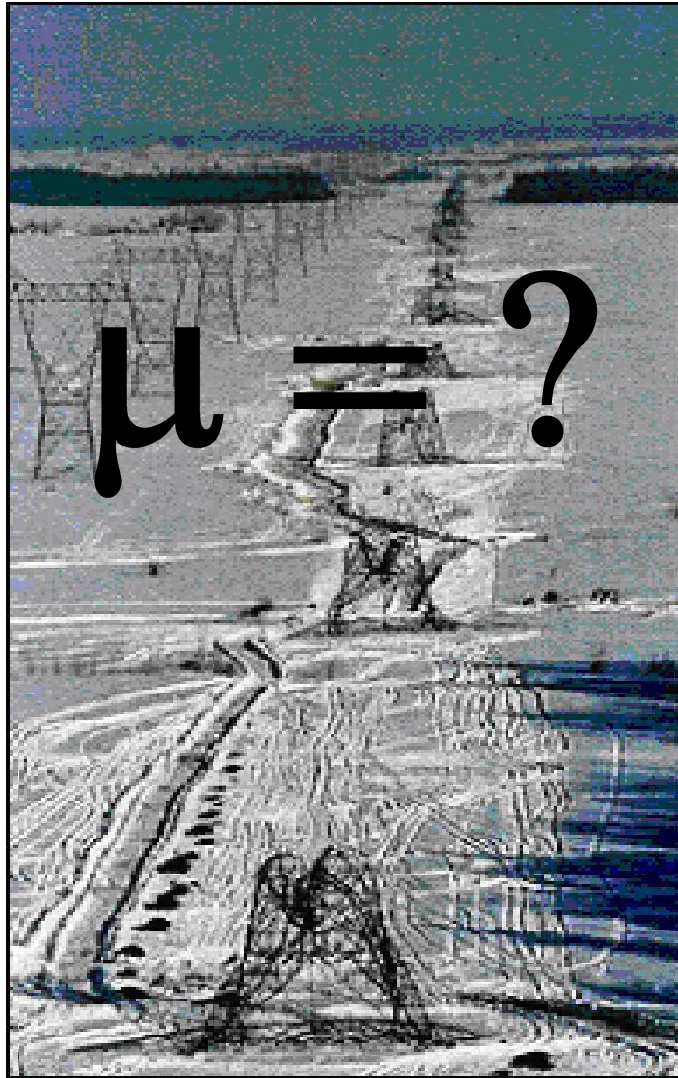
5

6

7 A. Please refer to PUB-NLH-187, Attachment 1 for the report titled *Assessment of Optimum Design*
8 *Return Period (RP) of a Proposed \pm 450 kV HVdc Line*, November 2009. As noted in Hydro's
9 response to NP-NLH-003¹ of the Reliability and Resource Adequacy Study proceeding, this draft
10 assessment was prepared by Dr. Haldar in 2009. The report was not finalized for use as a
11 baseline document for design.

¹ Filed with the Board of Commissioners of Public Utilities on August 13, 2020.

Assessment of Optimum Design Return Period (RP) of a Proposed ± 450 kV HVdc Line



Prepared by

Asim Haldar, Ph. D, P.Eng.
Manager of Engineering
Research and Development
Engineering Services

Prepared for

NE – LCP
WTO # DC1081
November, 2009

Assessment of Optimum Design Return Period (RP) of a Proposed \pm 450 kV HVdc Line System

Prepared by

Asim Haldar
Manager of Engineering
Research and Development
Engineering Services

Prepared for
Nalcor Energy – Lower Churchill Project
WTO # DC1081

Abstract

The report presents a systematic methodology in determining the optimum design return period of a proposed \pm 450 kV HVdc line. The method uses the initial line cost which depends on the selected return period value chosen. For each return period value selected, a corresponding failure rate is determined and a number of repair days are assumed depending on the degree and extent of the HVdc line failure event.

A system model based on a probabilistic planning approach is developed. It idealizes the Hydro's existing 230 kV system identifying the HVdc line as a generation source. The adequacy indices are determined using an approximate "frequency and duration" computation methodology.

Considering both the severity index and the unsupplied energy cost, it appears that a design return period of 150 years with a 50 MW gas turbine unit added to the system will be the least cost option that will optimize the total line cost and also satisfy the system adequacy criteria assumed in this study.

It is to be noted that the present study did not consider the submarine cable system and the converter stations, in developing the system reliability model. Adding these two subsystems will increase the severity index further and may lead to the choice of a line design based on a higher return period ($>$ 150 years) with additional generation support. This component has not been studied and should be considered seriously to achieve the best cost effective design of the entire HVdc line system.

Acknowledgements

The author would like thank Mr. Peter Thomas and Mr. Bob Moulton, System Planning Specialists, and Mr. Paul Stratton, System Planning department for their help on this project. Peter was instrumental in providing the load forecast as well as many other important input parameters during the development of this study. I also appreciate the assistance of Mr. Art Bursey, Sr. System Operation Engineer, System Operation Department in providing the operational data for plant equipment.

The model development tasks carried out by engineering students Christopher Willette, Stephen Reddin, Brent Peddle and Brad Tooktoshina are acknowledged here. These students developed the line cost model (**LCOST**) for the HVdc line system and the model for the cost of losses (**ECOST**) for the Island System. I would also like to acknowledge the help of Doug Maloney, Johnathan Walsh and Kyle Tucker from LCP (Lower Churchill Project) for providing the line cost estimate.

Finally I would like to thank Professor Roy Billinton to provide me a number of reference papers in the subject area of system adequacy model and specific helps with particular reference to data model on composite customer damage function (CCDF) and its application to reliability worth evaluation.

Table of Contents

1.0	Introduction.....	1
1.1	Project Background	1
1.1.1	Lower Churchill Hydroelectric Generation Project	1
1.1.2	Labrador - Island Transmission Link.....	2
1.2	Purpose of the Study-Background Information	5
1.3	Potential Market Additions	6
1.3	Scope	7
1.4	Section Layout.....	8
2.0	Line Failures	10
2.1	Line Failures in NLH System	11
2.2	Line Failures in HQ System.....	13
2.3	Line Failures in Manitoba Hydro (MH) System	14
2.4	Line Failures in Electricity de France (EDF)	15
3.0	Methodology	16
3.1	Simple Cost Equation	16
3.1.1	LCOST.....	17
3.1.2	ECOST	17
4.0	System Model.....	20
4.1	Probabilistic Model	24
4.1.1	Markov Model.....	24
4.1.2	Significance of Repair Rate Parameter (μ).....	26
4.1.3	Frequency and Duration Method (Billinton and Zhang, 1997).....	27
4.2	Load Model.....	29
4.2.1	Load Forecast (2016-31)	31
4.2.2	Planning Horizons (2016-31)	32
4.2.3	Bulk Indices for Electric Power System.....	33
4.3	Model Development - Bulk Electric Power System	37
4.3.1	Model Assumptions	39
4.4	System Indices Evaluation - Equivalent Model.....	41
5.0	Line Cost Model (LCOST).....	45
5.1	Framework for Developing Initial Line Cost	46
5.1.1	Environmental Line Loading	48
5.2	Suspension (Tangent) Tower -Cost Model	50
5.3	Strain (Dead End) Tower-Cost Model.....	52
5.4	Conductor Cost Model.....	55
5.5	LCOST Model (Equation 3.1 in Section 3.0).....	55

6.0	ECOST Model (Equation 3.1 in Section 3.0).....	59
7.0	Results (Base Model without GT)	65
7.1	System SI for Base Model ($\lambda = 0.02$, $\mu = 52$)	66
7.2	Sensitivity Study	66
7.2.1	Line Failure Rate (λ)	68
7.2.2	HVdc Line Repair Rate (μ)	69
7.2.3	Planning Horizon (15 years versus 50 years)	70
7.2.4	IEAR parameter	71
7.2.4.1	Discount Rates	72
7.2.5	Cost of Line Replacement (CR)	73
7.3	Cost Optimization (15 years & 50 Years).....	73
7.4	Cost Benefit Ratio (CBR) Analysis	75
8.0	Base Model with GT	76
8.1	Severity Index.....	76
8.2	ECOST	78
8.3	Cost Benefit Ratio (CBR).....	78
8.4	Comparative Assessment (Base Model and Base Model with GT)	80
9.0	Summary and Conclusions	83
10.0	Recommendations.....	85
11.0	References	86
12.0	APPENDIX (Typical Input Data).....	88

List of Tables

Table 4.1 – Projected System Peak Load and Installed Capacity	32
Table 5.1 – Segment Maximum Ice Loading for Various Return Periods	48
Table 5.2 – Maximum Wind Loading for Various Return Periods	49
Table 5.3 – Combined Wind and Ice Loads	49
Table 5.4 – Suspension Tower Weights in Three Segments.....	52
Table 5.5 – Dead End Tower Weight & Cost.....	54
Table 5.6 – Dead End Tower Weight & Unit Cost	54
Table 5.7 – Dead End Tower Weight & Unit Cost	55
Table 5.8 – Conductor and Shield Wire–Material plus Installation Costs	55
Table 5.9 – 50 Year Tower Unit Costs (CS_i & CD_{ij})	57
Table 5.10 – 50 year Tower Quantity Matrix for Various Line Segments (ns_i & nd_{ij}).	57
Table 5.11 – Total Cost for Selected Return Periods (2008\$).....	58
Table 6.1 – Customer Interruption Data (Base Case, Billinton, 1991\$/KW)	60
Table 6.2 – CCDF (1991\$*)	61
Table 7.1 – Sensitivity Study-Parameters	67
Table 7.2 – Sensitivity Study-Parameters	68
Table 8.1 – Comparative Assessment (Total Cost and Severity Index)	81

List of Figures

Figure 1.1 – Proposed Layout of Lower Churchill Project	3
Figure 1.2 – Proposed HVdc Route over the Long Range Mountains.....	4
Figure 1.3 – Cost Risk Model.....	7
Figure 2.1 – Observed Rime Icing Event on the Long Range Mountains.....	10
Figure 2.2 – Glaze Ice Sample from Conductor (1984 Storm)	11
Figure 2.3 – Large Angle Tower Failure near Hawke Hill (1988 Storm)	12
Figure 2.4 – A 735kV Line Cascade.....	13
Figure 2.5 – DC Tower Failure under Microburst (High Intensity Wind)	14
Figure 2.6 – Tower Failure in EDF System (Storm 1999).....	15
Figure 3.1 – Optimum Cost Risk Diagram.....	19
Figure 3.2 – Flow Diagram for Developing Cost Models	19
Figure 4.1 – System Reliability Sketch (Billinton and Allan, 1987)	20
Figure 4.2 – Typical Generation Model (Billinton and Allan, 1987).....	21
Figure 4.3 – State Space Diagram of a Power System with n-components (Zhang, 1995).....	23
Figure 4.4 – A Simple Two State Model	24
Figure 4.5 – A Simple Two State Markov Diagram	24
Figure 4.6 – Simple Four States Markov Diagram (Li, 2005)	25
Figure 4.7 – A Simple Bridge Failure.....	26
Figure 4.8 – Major Cascade Failure	27
Figure 4.9 – Time History of Load	29
Figure 4.10 – Hourly Load Duration Curve.....	30
Figure 4.11 – Typical Load Duration Curve.....	30
Figure 4.12 – Comparison of System Peak Loads and Installed Capacity	32
Figure 4.13 – Comparison of DUPI Data (CEA Report, 2005)	35
Figure 4.14 – Newfoundland and Labrador Hydro’s 230 KV Line System.....	38
Figure 4.15 – Single Line Diagram of the Island’s Bulk Electric Power System at 230kV Level	39
Figure 4.16 – Schematic Diagram for IA and AI	42

Figure 4.17 – Sketch Showing the IA and AI (Zhang, 1995)	42
Figure 4.18 – Sketch Showing a Typical State Condition.....	43
Figure 4.19 – Sketch Showing the Interconnected Area	44
Figure 4.20 – Sketch Showing the Area of Interest	44
Figure 5.1 – Typical Line Layout	45
Figure 5.2 – Typical Line Components.....	47
Figure 5.3 – Typical HVDC Suspension Tower	50
Figure 5.4 – Typical Dead End Tower (Reddin, 2009)	53
Figure 5.5 – Initial Line Costs with Respect to Various Design Return Periods	58
Figure 6.1 – Customer Distribution.....	60
Figure 6.2 – Customer Damage Function	61
Figure 6.3 – Composite Customer Damage Function (CCDF)	62
Figure 7.1 – Comparison of Severity Index (RP=50 years, MTTR=7 days).....	66
Figure 7.2 – Comparison of Severity Index (RP=50 years, MTTR=7 days).....	67
Figure 7.3 – Comparison of Severity Index for Various Return Periods	68
Figure 7.4a – Comparison of Severity Index for Various Repair Rates	69
Figure 7.4b – Comparison of Severity Index for Various Repair Rates	70
Figure 7.5 – Comparison of Present Values of Unsupplied Energy Cost	71
Figure 7.6 – Sensitivity of Present Values of Unsupplied Energy Costs	72
Figure 7.7 – Sensitivity of Present Values of Unsupplied Energy Costs	72
Figure 7.8 – Sensitivity of Present Values of C_f	73
Figure 7.9 – Cost–Risk Plot for Various Return Periods.....	74
Figure 7.10 – Cost–Risk Plot for Various Return Periods.....	74
Figure 7.11 – Cost Benefit Ratio for Two Different Return Periods	75
Figure 8.1 – Schematic Line Diagram with GT (East Bus)	76
Figure 8.2 – Comparison of Severity Indices with GT added to the System.....	77
Figure 8.3 – Comparison of Severity Indices with GT Added to the System	77
Figure 8.4 – Comparison of ECOST with GT for Two Planning Horizons	78
Figure 8.5 – Comparison of CBR for Two Different Return Periods	79
Figure 8.6 – Comparison of Base Model and Base Model with GT (RT=20 days)	80
Figure 8.7 – Comparison of Base Model and Base Model with 50MW GT.....	81

List of Symbols

λ = failure rate

μ = repair rate

L_i = load curtailment

d_i = duration

f_i = frequency of outage

C_T = total Cost

C_I = initial cost

PV = present value

NPV = net present value

n = number of states

i = net discount rate

$p_{s,i}$ = state probability

EDLC = Expected duration of load curtailment

EENS = Expected Energy not Supplied

SI = Severity Index

L_P = System Peak Load

$c(d_i)$ = cost per unit duration obtained from CCDF table

p_f = probability of failure

C_R = cost of replacement of line section

C_f = cost of failure

t = duration in hours

α_i = fraction of time on average a load is in excess of a specified value

MTTR= mean time to repair

RT= repair time

MTBF = mean time between failure

ECOST= cost of unsupplied energy

IEAR = weighted energy cost considering sector distribution

CDF = customer damage function

CCDF = composite customer damage function

T = return period

BEPS =Bulk Electric Power System

1.0 Introduction¹

1.1 Project Background

1.1.1 Lower Churchill Hydroelectric Generation Project

The Churchill River in Labrador is a significant source of renewable, clean electrical energy; however the potential of this river has yet to be fully developed. The existing 5,428 MW Churchill Falls generating station, which began producing power in 1971, harnesses about 65 per cent of the potential generating capacity of the river. The remaining 35 per cent is located at two sites on the lower Churchill River, known as the Lower Churchill Project.

The Lower Churchill Generation Project's two proposed installations, Gull Island and Muskrat Falls, will have a combined capacity of approximately 3,000 Megawatts (MW) and can provide 16.7 Terawatt hours (TWh) of electricity per year. That is enough to supply hundreds of thousands of households annually and contribute significantly to the reduction of air emissions from thermal, coal and fossil fuel power generation.

Along with these generation sites, interconnecting High Voltage Alternating Current (HVac) lines and associated infrastructure shall be constructed. These include:

- One double circuit 230 kV transmission line from the Gull Island Generation Site to the Muskrat Falls Generation Site.
- One single circuit 735 kV transmission line from the Gull Island Generation Site to the existing Upper Churchill Generation Site.

¹ Section information provided by John Walsh

1.1.2 Labrador - Island Transmission Link

The proposed 1,125 km High Voltage direct current (HVdc) link between Gull Island in Central Labrador and Soldiers Pond on the island's Avalon Peninsula will be the first of its kind in Newfoundland and Labrador. The link is part of a long-term solution to meet the province's clean energy requirements and its future economic development and growth.

The HVdc transmission system will be designed to deliver up to 750 MW (after losses) to the island. As currently planned, the \pm 450 kV HVdc transmission system will include:

- Overhead Transmission Line - Gull Island to Strait of Belle Isle
- Strait of Belle Isle Cable Crossing
- Overhead Transmission Line - Strait of Belle Isle to Avalon Peninsula
- Converter Stations at Gull Island and Soldiers Pond
- Electrodes

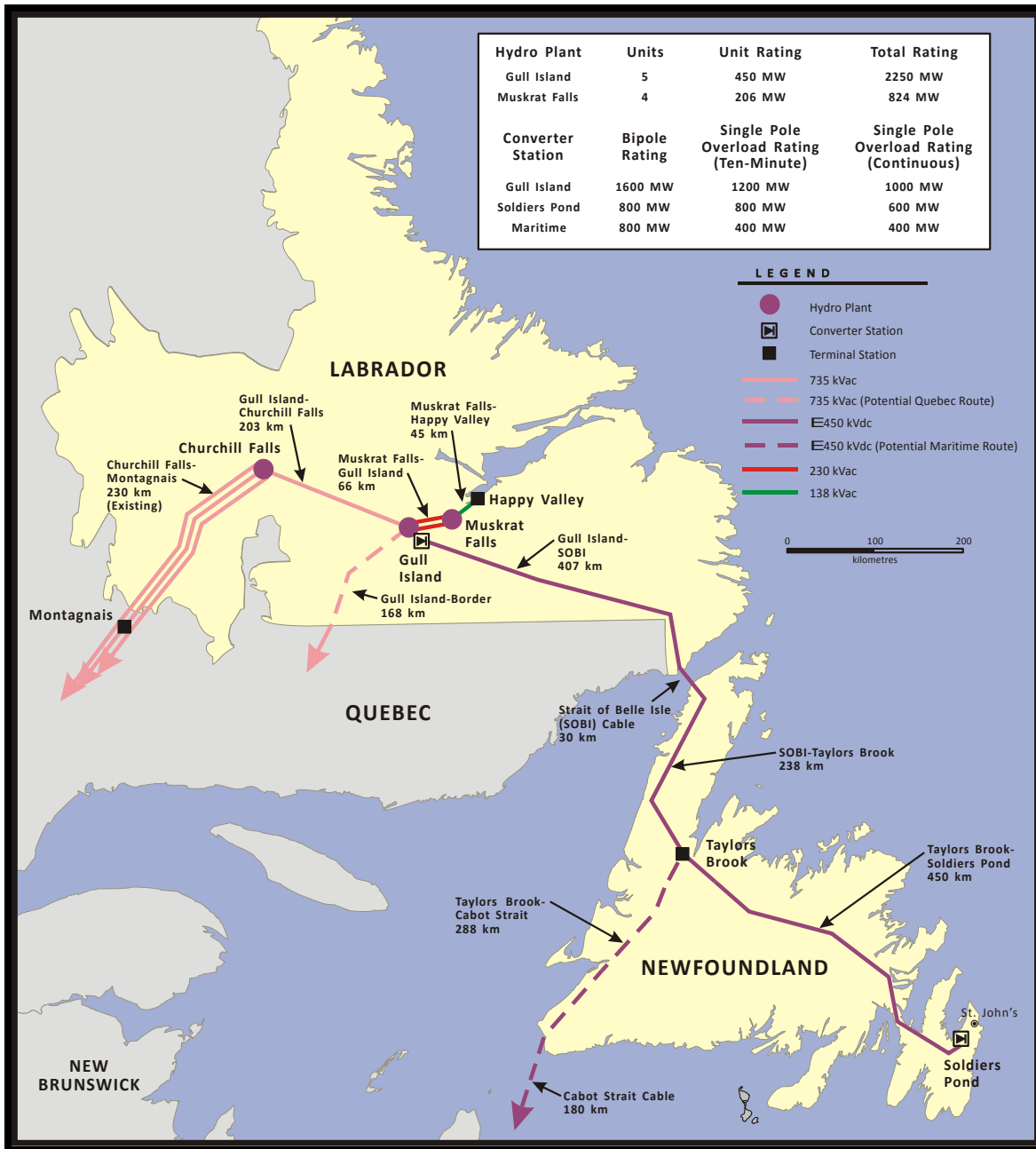


Figure 1.1 - Proposed Layout of Lower Churchill Project

The HVdc link to the island includes an underwater submarine cable system. In addition, the HVdc system will also have an option for a switching station near Taylors Brook for a multi-terminal scheme interconnecting with the Maritimes grid via submarine cables. Figure 1.1 presents the layout of this configuration. Part of this HVdc line will traverse the Long Range Mountains which is known for severe in-cloud glaze and rime icing conditions (Figure 1.2).



Figure 1.2 - Proposed HVdc Route over the Long Range Mountains

1.2 Purpose of the Study-Background Information

Current practices in the design of overhead lines for primary climatological loading are to use the return period concept where meteorological design loads such as wind, ice and combined wind and ice are prescribed with a specific return period value. In the utility industry, it is common practice to design major transmission lines to withstand a 50-year return period load. The return period of an event is the average time elapsed between occurrences. A wind speed with a 100-year return period called “100 year wind” will occur on average every 100 years. It will not necessarily be reached or exceed in the 100 year interval, or may even occur more than once in the same interval. A typical service (economic) life of 50 years is also assumed for a major transmission line. Prediction of the actual design value of a climatic event with a specific return period is an extremely difficult problem in lieu of the site specific data. Use of a 50-year design load within a service life of 50 years implies that the probability of exceedance is 64% (very high).

Some national and International standards prescribe the design load to be selected based on 50-year, 150-year or 500-year return period values depending on the importance of the line. A 50-year return period is normally selected for line design but a larger return period value can be selected if the line is an extremely important one. Therefore, the line design engineer may chose a higher return period such as 500 years to reduce the probability of exceedance to 10% level. It is also known that the capital cost of a line increases significantly as the selected value of the return period increases.

During the preparation of the Avalon upgrade study report (Haldar, 1995), the author raised the question as to how does one determine the value of “reliability worth”. To assess the “reliability worth value” one needs to include the failure costs explicitly. At the time, the total damage cost was assumed to be the fixed replacement cost for a failed section of a line. It was clearly pointed out in the report that the upgrading cost of the transmission line system on the Avalon Peninsula could not be justified unless it can be shown that the benefit derived from such an upgrade is economically viable.

However, it was also recognized at the time that a more detailed approach is needed to assess this “reliability worth” issue including customer interruption costs.

Since the completion of the Avalon upgrade study report and the subsequent completion of the Avalon upgrading capital project (1999-2005), the author has worked with CEATI WISMIG (Wind and Ice Storm Mitigation Interest Group) members to identify the need for developing a more robust model to integrate both the capital cost of new/or upgraded line with the customer interruption costs (outage costs) to assess the reliability worth value. A Task Force was formed in 2008 to undertake the study “Transmission line Failure Costs and its Impact on Line Design (CEATI Project 3347)”. The professional service of Professor Roy Billinton was retained to develop the composite customer damage function (CCDF) model for integrating the customer damage cost in the overall cost model.

On May 23, 2008, the author made a presentation to the members of the Lower Churchill design team with a suggestion that the selection of a 500-year return period or any return period which is significantly larger than the 50-year return period value should only be done if it can be shown quantitatively that the failure of the HVdc line will have a significant impact on the Newfoundland and Labrador Hydro’s (NLH) system. A methodology was outlined during this presentation to include the damage cost in terms of unsupplied energy and how this can be included in the cost optimization process. Subsequently, a Work Task Order (WTO) was issued in June of 2008 and the current study was initiated.

1.3 Potential Market Additions

Depending on the final market solution for the delivery of Lower Churchill Project power to market, several transmission options exist. At this time the market solution has not been finalized. Therefore optimum routing and planning will be decided in detailed design. The options include:

- Further HVdc overhead line to the west coast of Newfoundland and a Submarine Cable system to the Maritimes.
- One 735 kV Single Circuit Line from the Gull Island Generation Site into Quebec.

1.3 Scope

The scope of this study is to determine the optimum design return period of the HVdc line system by balancing the initial cost of the line against the present value of future failure costs.

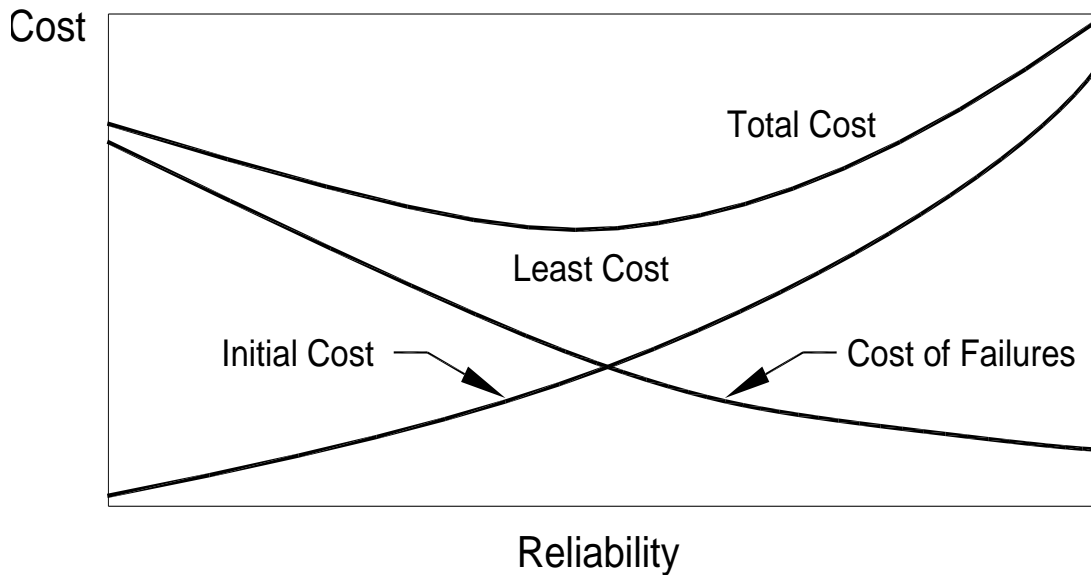


Figure 1.3 - Cost Risk Model

A methodology is developed based on a probabilistic system model where various system state contingencies are evaluated and its impact assessed in terms of a cost-risk model. Figure 1.3 depicts the saddle point where the total cost is minimized.

1.4 Section Layout

- Section 1 provides background information on the Lower Churchill project development.
- Section 2 provides some major historical line failure information that has happened in various utilities around the world.
- Section 3 describes the basic methodology.
- Section 4 presents the system model development to assess the unsupplied energy based on the island's 230 kV system and the HVdc Infeed.
- Section 5 presents the **LCOST** model.
- Section 6 presents the **ECOST** model.
- Section 7 presents the results from the base model and the sensitivity of key parameters.
- Section 8 presents the results from the base model with additional support such as gas turbine.
- Section 9 discusses the results and summarizes the conclusions.
- Section 10 lists the recommendations for future work.
- Section 11 presents the key references.

- Section 12 presents the Appendix and provides a typical data sheet for running the model.

2.0 Line Failures

Nalcor Energy operates approximately 5300 km of transmission line operating at the 69 kV, 138 kV, 230 kV and 735 kV voltage levels. The transmission network system consists of wood pole as well as steel and aluminum tower lines. Given the vast region covered by the transmission system, it is exposed to a severe harsh, cold environment. Most low pressure storm systems moving across North America, particularly on the eastern seaboard, pass over Newfoundland (Figure 1.1) and result in heavy precipitation (freezing rain or snow) with strong wind conditions. These maritime storms stall for a day or two and quite often deposit heavy freezing precipitation or snow during the winter months, which create significant operational challenges in maintaining the overhead transmission line system in Newfoundland and Labrador.

To study the icing phenomenon along the proposed HVdc transmission line route, Newfoundland and Labrador Hydro (NLH) installed a number of ice monitoring test stations (test spans and guyed towers at specific locations along the route) and operated these stations from 1977-1987. Figure 2.1 depicts a typical icing event that was observed on a test tower located on the top of the Long Range Mountains, and on the coast of Labrador.

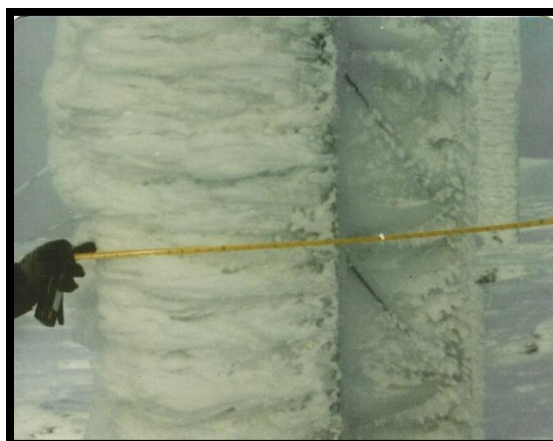


Figure 2.1 - Observed Rime Icing Event on the Long Range Mountains

2.1 Line Failures in NLH System

Since the commissioning of its transmission lines in the 60's, many parts of NLH's system have experienced multiple ice storms and severe ice loadings. The original design wind and ice loads for these lines were based on CSA (Canadian Standards Association) heavy load, which was 12.5 mm glaze ice combined with 117 km/hr wind with appropriate overload factors. Upon review of the pertinent information available at the time, two basic load conditions evolved: Normal Zone with 25.4 mm radial glaze ice and Ice Zone with 38 mm radial glaze ice. The Ice Zone was used for a small section of the transmission line system. The overload factor for all metal tower design was 1.33 while for wood pole structure, this factor was 2.0.

Several large ice accumulations have been observed. Since 1965, there have been at least four (4) major line failures on the Avalon Peninsula (eastern part of Newfoundland, Figure 1). Similar line failures have also been observed in other parts of Newfoundland (Haldar, 1990) including the Buchans Plain, located in the western part of Newfoundland (elevation 600 m above MSL (Mean Sea level), Figure 1.2). The line failures on the Avalon Peninsula occurred in 1970, 1984, 1988 and 1994 (Haldar, 1995). Figure 2.2 depicts the observed glaze ice sample on the conductor during the 1984 failure. The ice sample weighed approximately 7.8 kg/m.



Figure 2.2 - Glaze Ice Sample from Conductor (1984 Storm)

Figure 2.3 depicts the failure of a 230 kV heavy angle tower (self supported) in 1988 ice storm. In all cases, the lines experienced conductor/hardware failures due to ice overload. In this case, the line experienced a cascade where a few suspension guyed-v towers and the heavy angle strain tower were lost.



Figure 2.3 – Large Angle Tower Failure near Hawke Hill (1988 Storm)

The 1994 line failure caused a cascading event in which seven (7) H-frame wood pole structures (230 kV) were lost due to the failure of a forged eye bolt on a dead end structure. The replacement cost of the failed section of this line alone was approximately \$500,000 dollars. In 1970 and in 1984, NLH incurred several million dollars in repair and replacement costs and a long forced outage time before the system was brought back into operation.

In 1995, a detailed failure investigation study concluded that the steel transmission line system on the Avalon Peninsula needed to be upgraded to withstand a much higher ice load (66 mm radial glaze ice instead of a 25 mm radial ice load designed originally) and a major upgrading project was launched in 1998 to complete this work in 2003 (Haldar, 1995, 2006).

2.2 Line Failures in HQ System

During the first week of January 1998, the transmission network in southern and western Quebec was subjected to a severe freezing rain storm event which covered 150000 km² and affected 1.5 million customers from a few hours to 30 days in the provinces of Quebec and Ontario. Among installations rated 49 kV and above, over 2,000 wood portal structures and 617 steel lattice towers were destroyed or sustained significant damage. There were eight major cascade collapses among structures of the 735 kV transmission network. Figure 2.4 presents the 735 kV line cascade caused by the 1998 ice storm in Quebec.



Figure 2.4 – A 735 kV Line Cascade

Following the 1998 ice storm in Canada, Hydro-Québec drew up a three-part intervention strategy

- Emergency restoration of critical lines;
- Restoration of collapsed lines before the next winter peak;
- Reinforcement of the transmission system over the medium and long term.

2.3 Line Failures in Manitoba Hydro (MH) System

In the early hours of September 5, 1996 a severe thunderstorm moved through the rural area immediately northwest of Winnipeg. Nineteen guyed steel towers of the two parallel HVdc transmission line collapsed, causing the complete failure of the Radisson – Dorsey Transmission System carrying 2020 MW. In addition, another three steel towers and 18 wood pole structures were damaged. In spite of the extensive loss of power and damage, customers were not affected.



Figure 2.5 - dc Tower Failure under Microburst (High Intensity Wind)

The storm is believed to have been a microburst that produced extremely High Intensity down pressure and lateral Winds (HIW). The high winds moved through a narrow strip, approximately two km wide. Analysis of damage, supported by radar data, suggested that a straight line wind associated with a microburst storm occurred. Based on the damage evidence, it was estimated that low end F1 winds (116-179 km/h) occurred in the area. Since this line failure, MH has launched a major R & D project (more than 1 M\$) to study and understand better the effects of HIW on transmission lines. The final report will be published by the end of 2009.

2.4 Line Failures in Electricity de France (EDF)

In December 1999, France suffered two major storms bringing exceptionally high winds causing extensive damage to transmission and distribution networks. After the two storms 3,450,000 customers in 90 French districts were left without electricity. Within 24 hours, electricity was restored to 1,500,000 households. The last few customers were finally re-supplied on mid January, 2000. All the substations and industrial customers were reconnected in less than 4 days.



Figure 2.6 – Tower Failure in EDF System (Storm 1999)

In all, 70,000 people worked to re-establish service. Equipment resources were acquired in matching proportions: more than 5000 generator sets of all power levels, 2500 tons of supports, 4000 km of conductors and 900,000 connection parts were used. During the restoration, 11 emergency lines, including 4 from abroad, were installed on 8 links.

3.0 Methodology

The purpose of this study is to determine the optimum design return period of the HVdc line by balancing the initial line cost (**LCOST**) against the present value (PV) of future failure costs (**ECOST**). It is well known that the overestimation of the design wind and ice loads will significantly affect the initial design cost of a line, while the underestimation of these loads would certainly impose “future” failure costs which, in some instances, could be quite significant. Some examples of several recent major line failures are presented in Section 2.0 and their consequences. A typical line failure for a very small event could cost NLH \$500,000 dollars just to replace the damaged line (Avalon Study report, 1995), not including the customer interruption costs (commercial and business) and losses.

3.1 Simple Cost Equation

A methodology is developed based on a probabilistic system model where various system state contingencies are evaluated and the corresponding impacts assessed in terms of a cost-risk model. The mathematical expression is presented below

$$C_T = C_I + PV (\text{Future Failure Cost}) \quad [3.1]$$

where

C_T = total line cost (**TCOST**) based on a specific design return period, T and the present value of the future failure cost;

C_I = initial line cost (**LCOST**) which is a function of the design return period, T, of the climatological loading parameters such as wind, ice etc.

PV (future failure cost) = present value of future failure costs including repair/upgrade costs and customer interruptions costs

3.1.1 LCOST

The **LCOST** includes only the cost of line materials and construction. The costs associated with engineering, survey, camp site development etc. are not included because they are invariant to the design return period. The failure rate λ is directly related to return period, **T**.

3.1.2 ECOST

The net present value of the future failure cost has two components. (1) tangible cost and (2) intangible cost. The tangible cost normally includes the expected replacement cost of the line after a failure and the cost of expected energy not supplied (**EENS**). On the other hand, the intangible cost could be the increase in the future insurance premium, societal cost etc, which are difficult to quantify (Billinton and Allan, 1987) and is not included here.

$$\textit{Future Failure Cost} = C_f + \textit{ECOST} \quad [3.2]$$

where

$$C_f = P_f C_R \quad [3.3]$$

C_f = expected failure costs which primarily includes the replacement cost (C_R) of the line section that failed during an extreme event. This cost can be estimated reasonably based on the past data.

P_f = annual probability of failure

ECOST is the cost of expected energy not supplied during the failure event. Primarily, this cost can vary widely depending on the consequence of the failure on the system, customer distributions and hence the composite customer damage function (CCDF) normally expressed in \$/KWh (described in Section 6.0).

Total line cost (C_T) is a function of many important line design parameters which depend on the line failure rate, λ the repair rate μ , the direct cost of failure, C_f and the cost of energy not supplied, **ECOST**. The NPV (net present value) of the failure cost is determined based on the discount rate, service life of the asset and the annual cost (\$/year) estimated based on equations (3.2 and 3.3).

ECOST will also be dependent on the system load (peak versus durational), as well as the system state during a failure event. The state probability in this study is computed based on a probabilistic system approach.

Two basic scenarios are considered in developing the cost-risk model: (1) no additional generation support (gas turbines) and (2) with additional generation support (gas turbine added)

Figure 3.1 depicts the graphical representation of equation 3.1. The initial line cost will increase as the reliability increases, while the cost of losses will decrease with increasing line reliability. It is expected that an optimum region can be found by balancing these two costs. Figure 3.2 presents the flow diagram for developing various cost components. Two computer programs were developed during this study. These are: (1) **LCOST** and (2) **ECOST**. The background information will be described in Sections 4.0, 5.0 and 6.0 respectively.

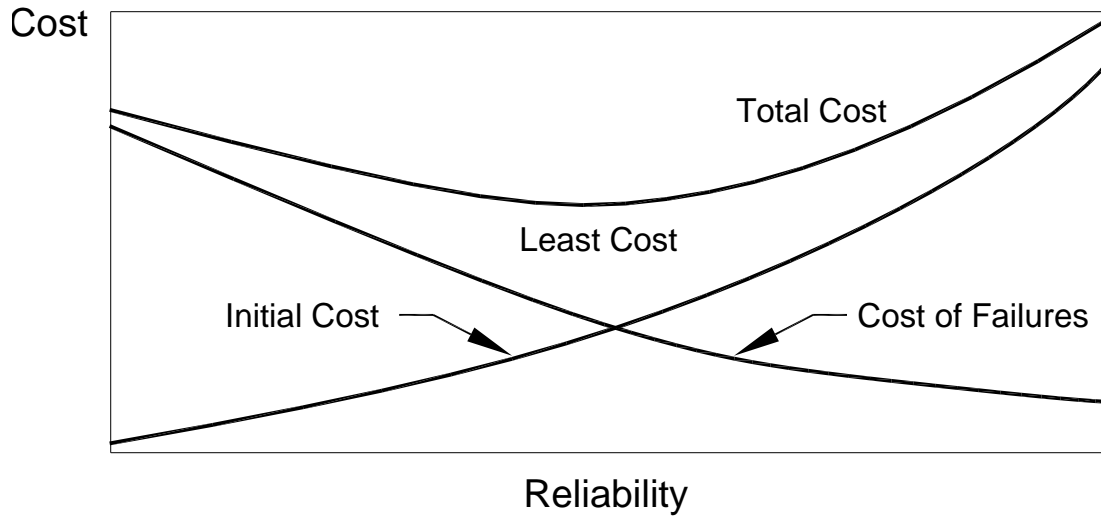


Figure 3.1 – Optimum Cost Risk Diagram

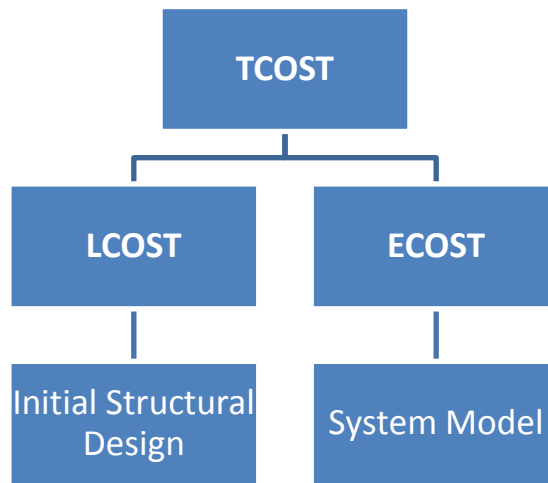


Figure 3.2 – Flow Diagram for Developing Cost Models

4.0 System Model

The primary function of an electric power system is to supply electrical energy to its customer economically with an adequate degree of reliability and service continuity. Billinton and Allan (1987) describe the system reliability in terms of system adequacy and system security. Adequacy refers to the system capacity to respond to its customer requirements (load demand) taking into account line constraints (voltage and thermal limits) as well as component outages. Security refers to the ability of the system to respond against transient disturbances (faults or unscheduled removal of components). Adequacy refers to “long term” planning criteria (steady state) while security relates to “short term” disturbances (dynamic situation) on the system. Figure 4.1 presents this in graphical form.

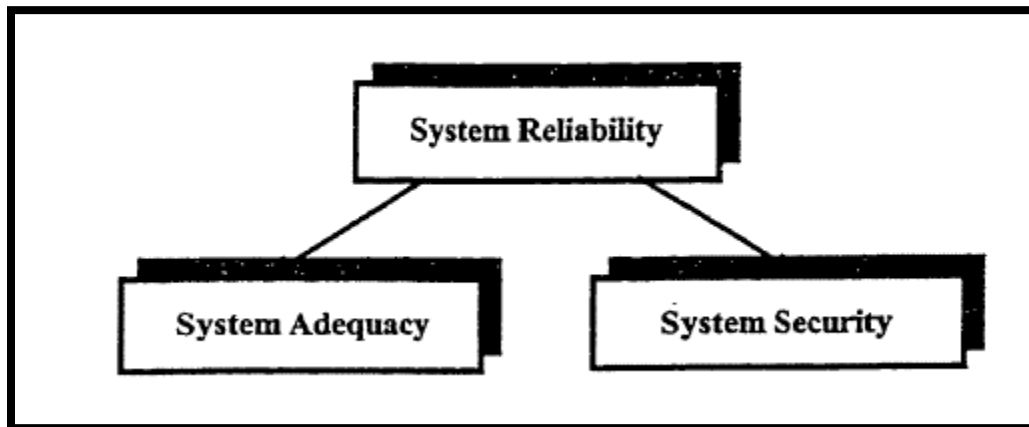


Figure 4.1 - System Reliability Sketch (Billinton and Allan, 1987)

The NLH System Planning Department uses the deterministic approach in planning the composite bulk electric power system (BEPS). The most common security criteria used in BEPS planning is **N-1 criterion** where it is assumed that the system should not have any outages if there is loss of a single BEPS component (such as a generating unit or a transmission line). The method uses a worst case scenario such as the peak load condition and the assumption is if the system can withstand the “worst case scenario” then it can withstand the remaining scenarios.

Some utilities also use **N-2 criterion** or **N-1-1 criterion** where it is assumed that the system should be able to withstand the loss of two components at a time or the forced outage of a single component in conjunction with scheduled maintenance of another component. Deterministic techniques are based on “subjective judgment”. The shortcoming of the deterministic method is that it is unable to produce a quantitative reliability measure and therefore, it is difficult to use in an economic analysis in an objective manner. The method also puts “hard limits” on equipment operation and, as a result, the systems are often designed to withstand severe events with low probability of occurrence. Although the deterministic criteria can not produce the “risk index” for a BEPS, their application is simple and easy to understand and interpret. Figure 4.2 presents the typical deterministic model for generation planning where the adequacy indices are typically defined as LOLP (Loss of Load Probability), LOLE (Loss of Load Expectation) and unsupplied energy (UE) etc.

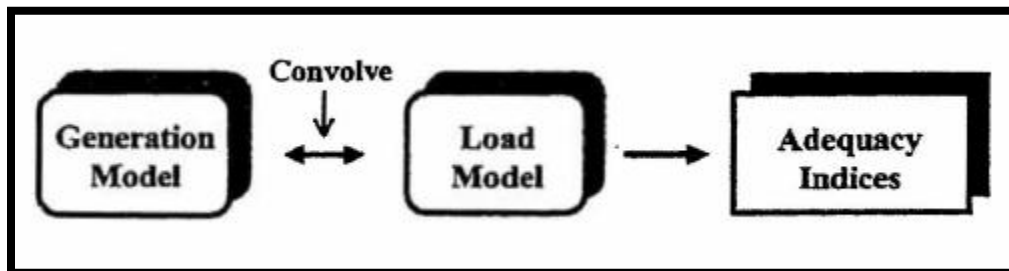


Figure 4.2 - Typical Generation Model (Billinton and Allan, 1987)

On the contrary, the probabilistic method explicitly takes into account the factors that may influence the system performance. It provides a quantitative measure of “risk” in terms of system performance indices such as probability and frequency of occurrence of an unacceptable event, duration and the severity of the events etc. The method is easily adaptable to the economic-decision making process and can provide an estimate of the energy not supplied or at risk. The method applied in this study can not only provide a quantitative measure of the various “risk indices” to measure BEPS adequacies but also provides a mechanism to integrate the system cost of losses in case of a failure event and allows this cost to be integrated with initial line cost in equation (3.1).

The probabilistic approach requires three steps to assess the system adequacy indices. These are: (1) system state (outage contingency) enumeration (2) analysis and (3) formation of bulk power indices. Later, these indices, particularly the unsupplied energy at risk, can be used with a customer damage function (developed from service sector data) to carry out an economic analysis which is more objective and realistic. The system indices are obtained after most of the system states have been considered. The system state can be obtained from a "Markov Model" which is very difficult to use for a practical composite power system where the number of components and the states could be very large.

In a general system with n-components having two simple states (availability or unavailability), the total system state would be 2^n (Figure 4.3). For a two component system, the system will have four states while for a BEPS with a generation plant having three units and two lines the total system states would be $2^5 = 128$. Not all states will have the same system impact but it is important to include as many of these states in the analysis to ensure that the sum of all system state probabilities are close to 1.0 or very high (0.999, 0.9999 etc.)

Since the number of states can be very large for a real system, it is important that we consider only those states which will have a significant impact on the system performance (load curtailment) rather than trying to include all states. The state selection level could be a fixed number of state levels (e.g. 4 states) with some restriction on the occurrence of the joint state probabilities below a threshold value (10^{-8}).

The challenge in the system adequacy problem evaluation is to understand the mechanism that causes a system problem. In a complex bulk power system, failure is assumed to have occurred when supply to the load buses is interrupted or the power quality is unacceptable. The following conditions could lead to this type of problem.

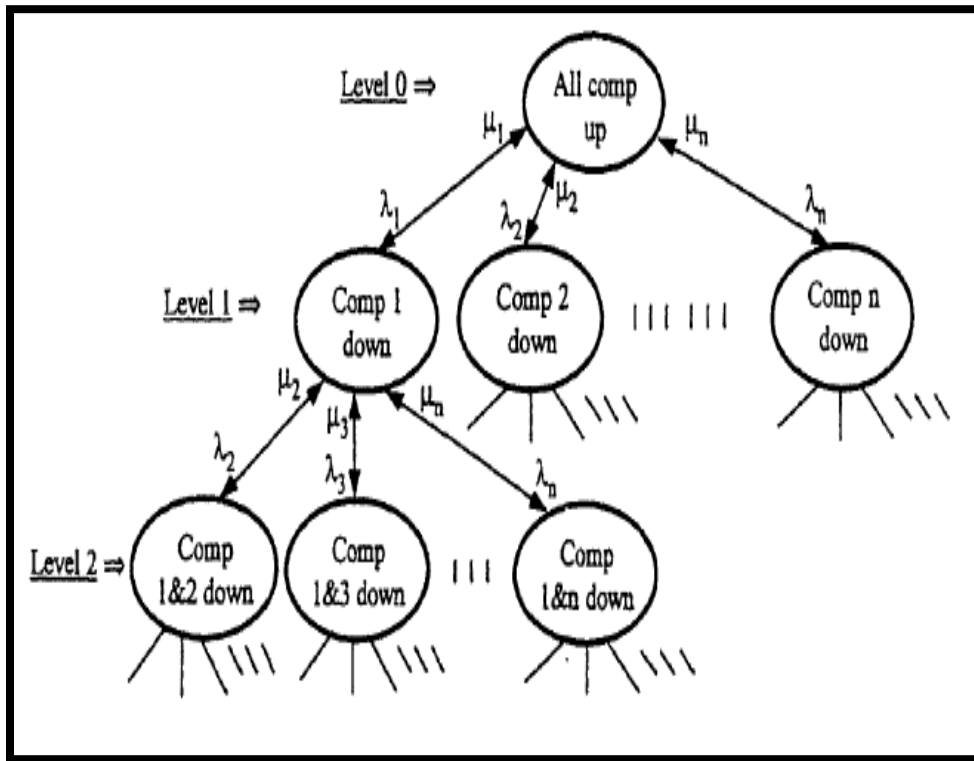


Figure 4.3 - State Space Diagram of a Power System with n -components (Zhang, 1995)

- Insufficient generation to meet the load demand
- Interruption of the power supply continuity
- Overloaded transmission lines
- Bus voltages are outside the tolerance levels

Most of the system problem arising from any one of the violations can be taken care of by security mitigation such as switching, generation rescheduling or load shedding. The system outage states which contribute to the voltage violation or load shedding after all the corrective actions have been taken contribute to the system adequacy indices.

4.1 Probabilistic Model

4.1.1 Markov Model

Figure 4.4 depicts a simple system with a generating unit and the bus load shown as demand.

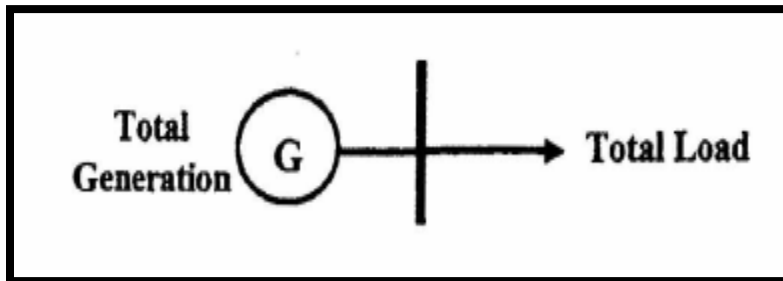


Figure 4.4 - A Simple Two State Model

For this one component system, the system has two states. The availability and the unavailability are computed as

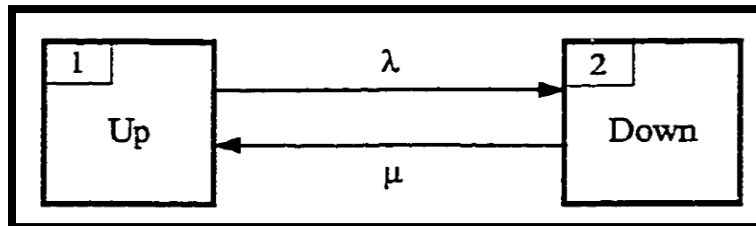


Figure 4.5 - A Simple Two State Markov Diagram

$$\text{Availability} = \frac{\mu}{\lambda + \mu} \quad [4.1]$$

$$\text{Unavailability} = \frac{\lambda}{\lambda + \mu} \quad [4.2]$$

where

λ = failure rate (occurrences per year)

μ = repair rate (repair occurrences per year)

For a two component system, the system has four states. The system state probability for both components down is given as (Billinton and Allan, 2007)

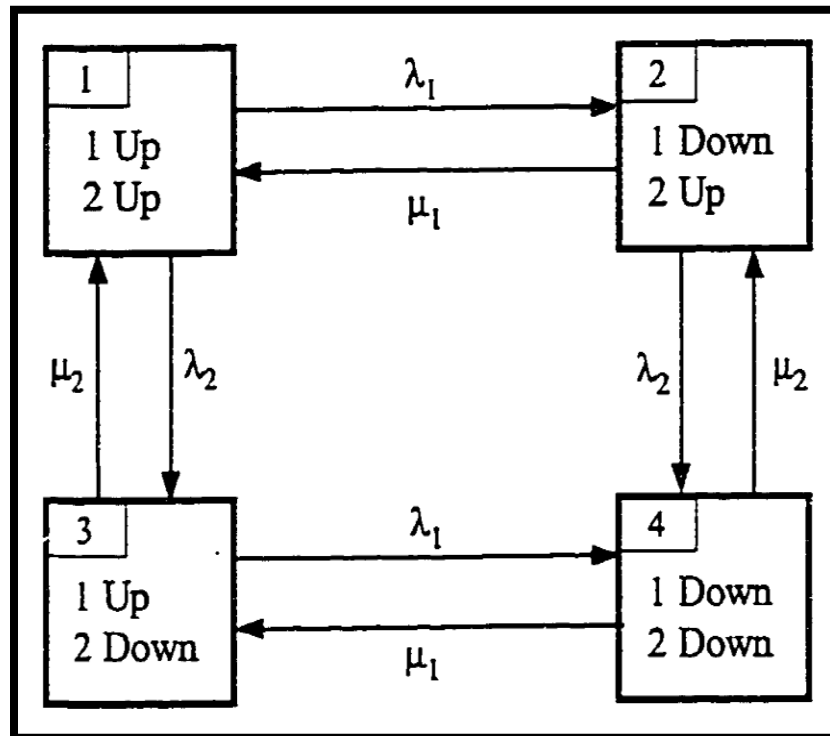


Figure 4.6 - Simple Four States Markov Diagram (Li, 2005)

$$\text{Unavailability (both down)} = \frac{\lambda_1 \lambda_2}{(\lambda_1 + \mu_1)(\lambda_2 + \mu_2)} \quad [4.3]$$

The above state probabilities are calculated based on a “Markov Model”. However, their application is limited for a system with many components and therefore, an approximate “frequency and duration” method developed by Billinton and Allan (1987) is used here to

determine the total system indices including generation and transmission. It is assumed that the component's failure modes are independent and this further simplifies the development of state space probabilities.

4.1.2 Significance of Repair Rate Parameter (μ)

The advantage of using this system model concept is that one can model the frequency and severity of the line failure through two parameters only, λ and μ respectively. For example, if the HVdc line has a crossarm failure due to ice overloading (Figure 4.7), it can be assumed that the line can be repaired quickly (1-3 days). This could be classified as low level failure and μ will reflect this condition. On the other hand, if there is a moderate to severe cascade failure (Figure 4.8), where many towers are lost, then the repair days could be significant (say 3-20 days) and μ could be adjusted accordingly to assess the impact on the system. A 3 day repair time implies a repair rate, μ would be 122.0 occurrences per year.

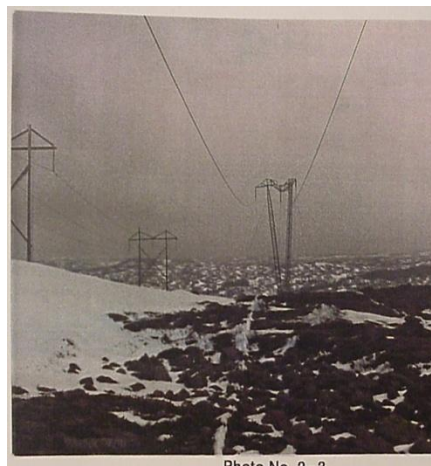


Figure 4.7 - A Simple Bridge Failure



Figure 4.8 - Major Cascade Failure

Typical line design only considers a fixed design return period. To the best of author's knowledge, this is the first time such a model is used to understand the simultaneous effects of the failure rate and repair rate parameters on total line cost

4.1.3 Frequency and Duration Method (Billinton and Zhang, 1997)

Assuming component independence, the system state probabilities and the failure and repair rates are computed by the equations

$$p_{si} = \prod_{k \in I} A_k \prod_{m \in O} U_m \quad [4.4]$$

$$\mu_{si} = \sum \mu_m \quad [4.5]$$

$$\lambda_{si} = \sum \lambda_k \quad [4.6]$$

where

I = set of in-service components in state, s_i

O = set of out of service components in state, s_i

A_k = availability of component, k

U_m = unavailability of component, m

λ_k and μ_m are the failure rate of component k and the repair rate of component m respectively. μ_{si} is the rate of repair and λ_{si} is the rate of departure at system state si respectively.

The system state frequency (occurrence/year) and the duration (hours) are computed from the following equations

$$f_{si} = p_{si} (\lambda_{si} + \mu_{si}) \quad [4.7]$$

$$d_{si} = \frac{p_{si}}{f_{si}} 8760 \quad [4.8]$$

The above calculation is based on a constant system load normally occurring for 8760 hours (one year). However, the system load is normally represented as hourly and therefore the load model should include the durational variation as well as the peak load (Figure 4.9). The next section describes the load modeling process.

4.2 Load Model

In developing the cost-risk model for this study, the System Planning Department was asked to provide a long term load growth forecast to ensure that the overall system with the HVdc line will be able to meet the adequacy requirement reliably. In the analysis, the HVdc line is used as a source and is assumed to provide 800 MW supply. Table 4.1 (on page 30) shows that beyond 2031, as the load grows there will be a considerable shortfall in system installed capacity and therefore, the present analysis was restricted to only 2031 load growth as shown in the Table 4.1 (Thomas,2009).

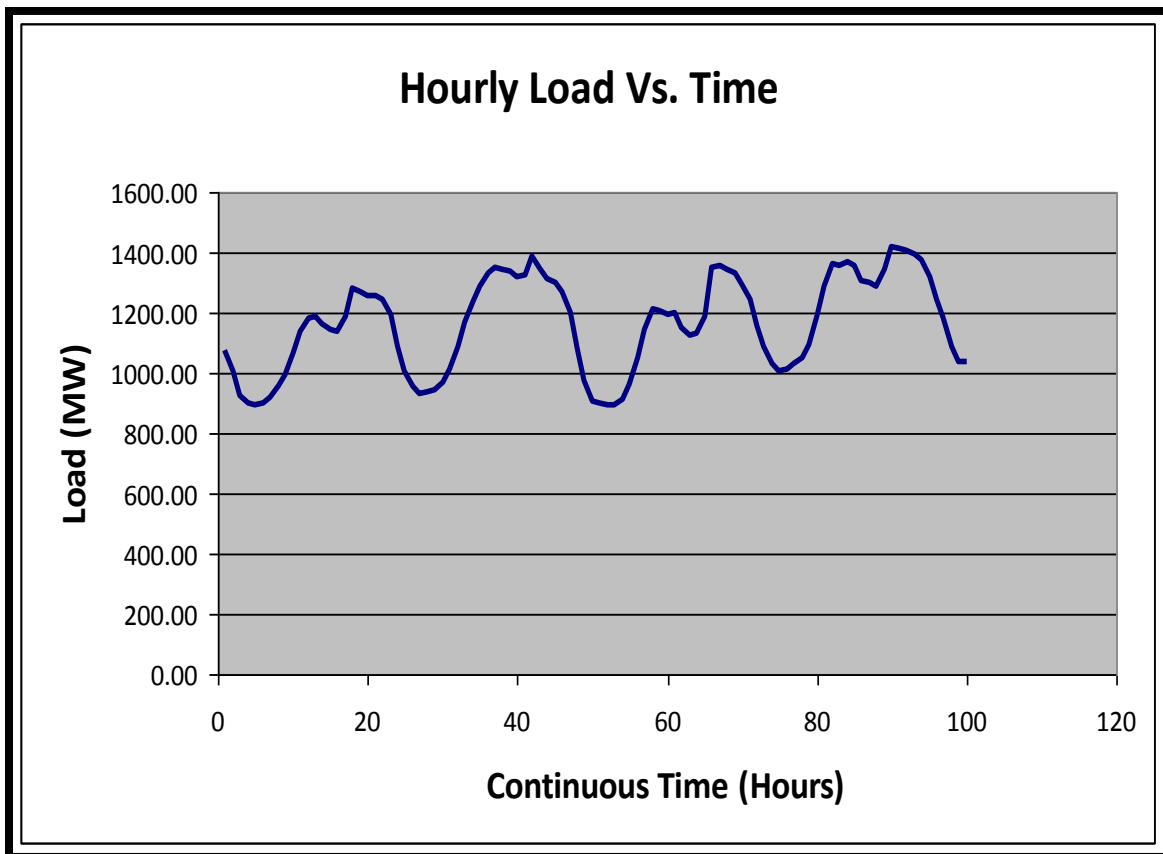


Figure 4.9 - Time History of Load

The system load can be measured in terms of peak load or can be modeled as hourly values (8760 hours) for the year. Figure 4.10 shows a snapshot of a forecasted load duration curve for 2016. The system peak load is 1508 MW and the horizontal axis shows the percentage of time the load will be above a certain value. Figure 4.11 shows that the hourly load duration can be discretized further in various load steps and the system adequacy analysis can be performed for each of these load steps.

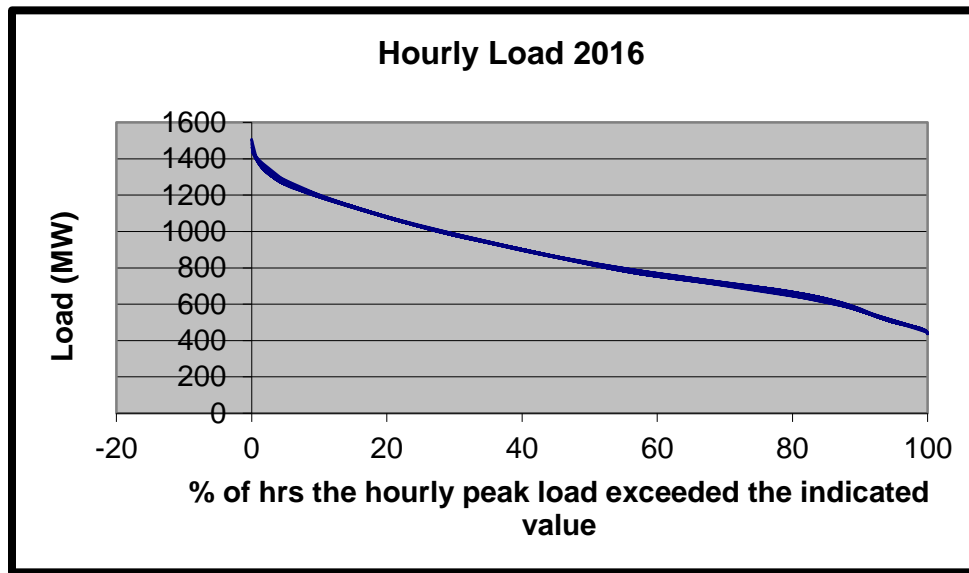


Figure 4.10 – Hourly Load Duration Curve

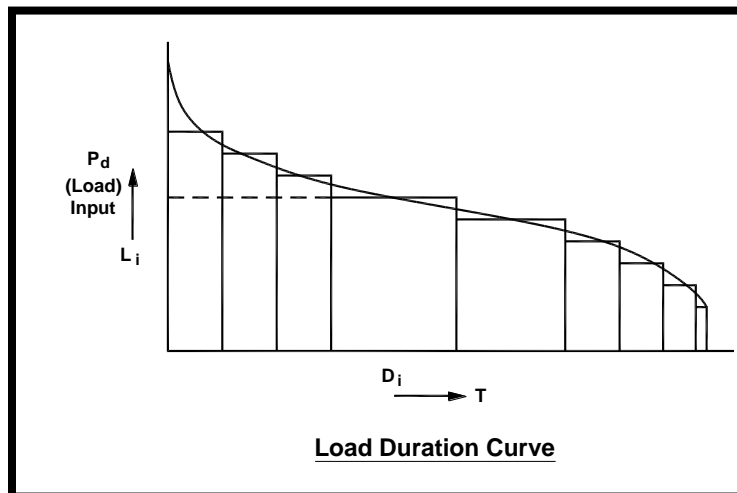


Figure 4.11 - Typical Load Duration Curve

A load level " L_i " with a time interval of " D_i " implies that the load, L_i falls in this interval. Therefore, the relative frequency of occurrence (or probability of occurrence of load level, L_i) is written as

$$\alpha_i = \frac{D_i}{t} \quad [4.9]$$

where $t = 8760$ hours;

If the probability of failure for load level L_i is P_{fi} , then the failure probability for the entire year can be obtained as

$$P_f = \sum_1^m \alpha_i P_{fi} \quad [4.10]$$

The annualized failure probability is based on constant load while the annual probability considers the load variation on a hourly basis and therefore is more representative for adequacy analysis (Billinton and Allan, 1987). This study uses annual values for all forecasted years beginning in 2016 with a 5-year interval to 2031.

4.2.1 Load Forecast (2016-31)

Based on the current installed capacity (Hydraulic plants), it was estimated that load forecast in year 2031 will provide an approximate 3% margin (Table 4.1). Figure 4.12 presents the data

Table 4.1- Projected System Peak Load and Installed Capacity

Year	Annual Peak Load (MW)	Generation Available in Model (MW)
2016	1508	1718
2021	1491	1718
2026	1577	1718
2031	1673	1718

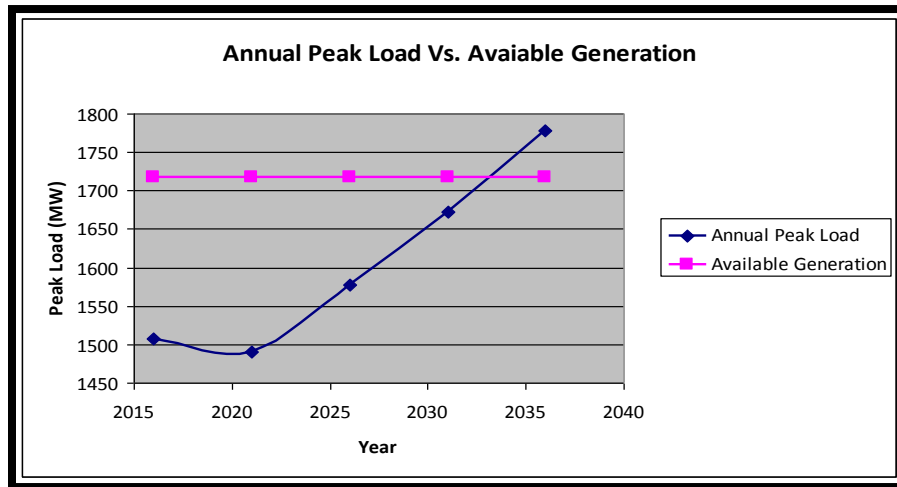


Figure 4.12 - Comparison of System Peak Loads and Installed Capacity

4.2.2 Planning Horizons (2016-31)

Beyond 2031, additional generation capacity is required to meet the load demand, which will require major capital expenditures. Therefore, the short term planning horizon is assumed to be 15 years assuming the HVdc line is commissioned in 2016. It is also assumed in the analysis that the Holyrood plant will be decommissioned in 2016 to coincide with the commissioning of HVdc line. However, a 15 year planning horizon is not realistic considering the large capital investment for HVdc line system and therefore, a standard 50 year service life was also considered to carry out the optimization study with the assumption that the load will be kept constant from 2031 until 2066.

Since the new generation resource development on the island beyond 2031 is not certain at this point and considering a large number of options that are available to Nalcor Energy to meet the demand beyond 2031, it was decided after a discussion with the System Planning Department that the load demand is kept constant beyond 2031 at this point (Thomas, 2009). This will simplify the current economic analysis although it is an exercise that the System Planning Department can undertake in the future to study the effects of this large capital investment beyond 2031 on the optimum design return period.

4.2.3 Bulk Indices for Electric Power System

$$\text{PLC} = \text{Probability of load curtailment} = \sum_{i=1}^S P_i \quad [4.11]$$

where P_i is the probability of system state, i and S is all states considered.

The system state frequency F_i is calculated by the following equation

$$F_i = P_i \sum_{k=1}^N \lambda_k \quad [4.12]$$

where λ_k is the departure rate (failure rate of component k) and N is the set of all components of the system.

The expected duration of load curtailment (**EDLC**)

$$\text{EDLC} = \text{PLC} \times 8760 \text{ hours} \quad [4.13]$$

The expected load curtailment (**ELC**)

$$\text{ELC} = \sum_{i=1}^S L_i F_i \quad (\text{MW} / \text{year}) \quad [4.14]$$

where L_i is the load curtailment (MW) in system state, i

The expected demand not supplied (**EDNS**)

$$\mathbf{EDNS (MW)} = \sum_{i=1}^S \mathbf{C}_i \mathbf{P}_i \quad [4.15]$$

The expected energy not supplied is (**EENS**)

$$\mathbf{EENS} = \sum_{i=1}^S \mathbf{L}_i \mathbf{P}_i \mathbf{d}_i \quad (\text{MW-hr/Year}) \quad [4.16]$$

Where \mathbf{d}_i is the duration of the system in state, i and

$\mathbf{d}_i = 8760 \times \mathbf{P}_i$ (hour) if the annualized value is sought or calculated based on discretized load duration curve if an annual value is sought.

The system severity index (SI) is computed by the equation

$$\begin{aligned} S_i &= \frac{\mathbf{EENS}}{\mathbf{LP}} \quad (\text{hour/year}) \\ &= 60 \frac{\mathbf{EENS}}{\mathbf{LP}} \quad (\text{minutes/year}) \end{aligned} \quad [4.17]$$

where

\mathbf{LP} is the annual system peak load in MW. The S_i index is also known as **DUPI** (delivery point unreliability index) as shown in Figure 4.13.

Figure 4.13 presents Canadian average and NLH average SI values reported for CEA study. The expected damage cost (**EDC**) for unsupplied energy is estimated based on composite customer damage function (**CCDF**)

$$EDC = \sum_{i=1}^S L_i f_i c(d_i) \quad [4.18]$$

where $c(d_i)$ is computed from **CCDF** (unit damage cost \$/kWh). The details on **CCDF** will be described in Section 6.0.

In this study, the last two parameters **SI** and **EDC (as part of ECOST)** will be used to assess the optimum design return period. The parameter EDC is the major component of the second term in equation 3.1.

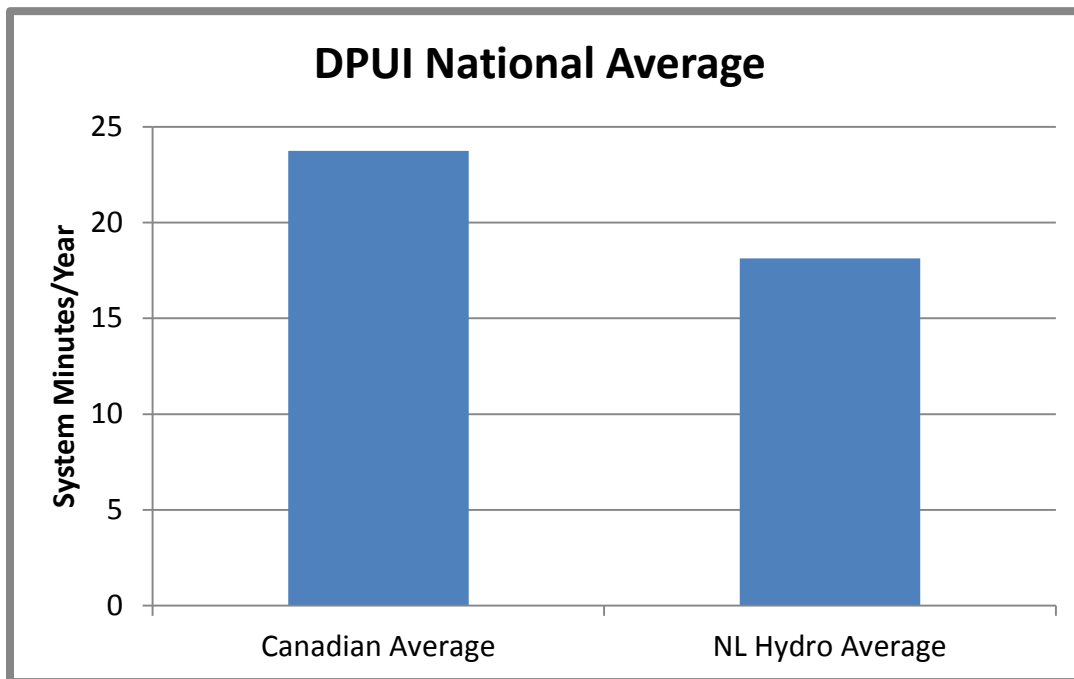


Figure 4.13 - Comparison of DUPI Data (CEA Report, 2005)

Billinton and Wangdee (2006) have recently compiled the CEA outage statistics data to provide delivery point unreliability indices (**DPUI**) and significant power interruptions (**SPI**). The paper summarizes the **SPI** data on bulk electric power system (BEPS) disturbance (widespread power interruption of 1 minute or more) and local network

interruption that may include major impact on customers due to duration or amount of load curtailed/affected) of 1000 MW-minutes or more. Table 4.2 provides a summary of the definitions and the indices classified.

The bulk electric power system (**BEPS**) disturbance is classified as follows:

- Loss of system stability
- Cascading Outages of Transmission Lines
- Abnormal range of frequency and/or voltage

The local disturbance is an event which results in an interruption of a local nature causing major customer interruptions due to duration or the amount of load affected. The measurement unit is MW-minutes.

**Table 4.2 - Degree of Severity for BEPS Disturbances and Local Disturbances
(Billinton and Wangdoe, 2006)**

Degree of security	Description	BES Disturbance (System Minutes)	Local Disturbance (MW-minutes)
Degree 0	-an unreliability condition normally considered acceptable	< 1	<1000
Degree 1	-an unreliability condition which may have significant impact to one or more customers but is not considered serious -typically the customer impact is less than 10 times above that which considered acceptable	1-9	1000-9999
Degree 2	-an unreliability condition which may have significant impact to one or more customers but is not considered serious -typically the customer impact is 10 to 100 times above that which considered acceptable	10-99	10,000-99,999
Degree 3	-a very serious impact to customers -typically customer impact is 100 times above that which is normally acceptable	\geq 100	\geq 100,000

In the cost optimization study, the severity index parameter and the degree of severity level specified in Table 4.2 will be used to develop the various cost risk options to select the option based on minimum cost.

4.3 Model Development - Bulk Electric Power System (NLH 230 kV System)

Figure 4.14 presents the Newfoundland and Labrador Hydro bulk power system at the 230 kV level. The transmission line system connects the major hydraulic generating stations. A conscious decision was made to include only the 230 kV line system with hydraulic plants to keep the model simple and to ensure that the model is easy to implement. The methodology is quite robust and can include other lines at the 138 kV and 69 kV levels but it is not necessary to include these lines at this stage. The objective here is to get a high level “cost risk” model first to understand the design risk consequences.

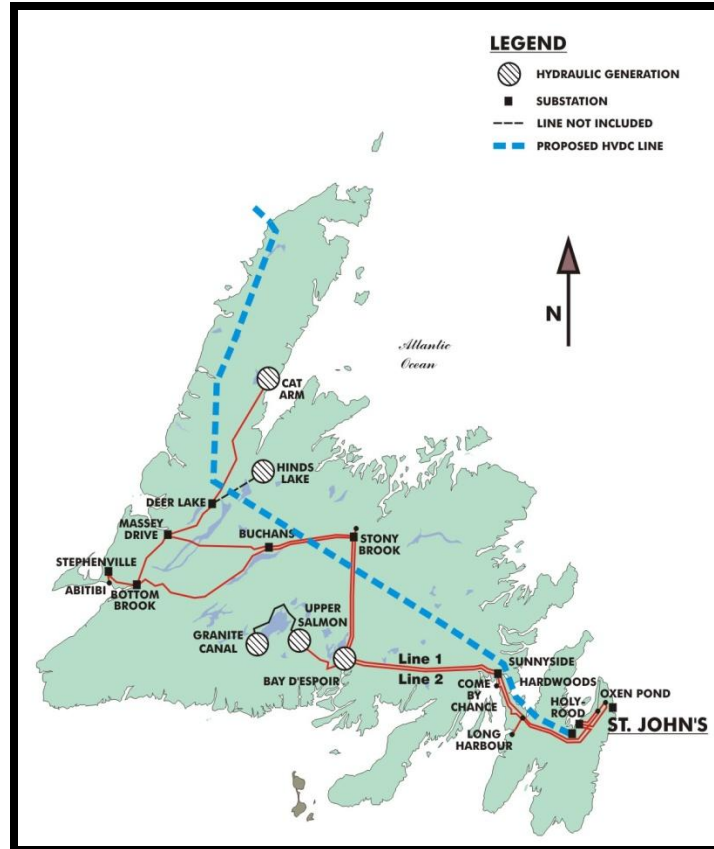


Figure 4.14 - Newfoundland and Labrador Hydro's 230 kV Line System

The basic 230 kV transmission line system primarily originates from Bay d'Espoir Generating Station and runs east and west. On the western part of the island there are two hydroelectric generating plants (Cat Arm and Hinds Lake) which also provide power to the network through high voltage lines. Figure 4.15 presents the single line diagram for 230 kV system which is used to develop the system reliability model.

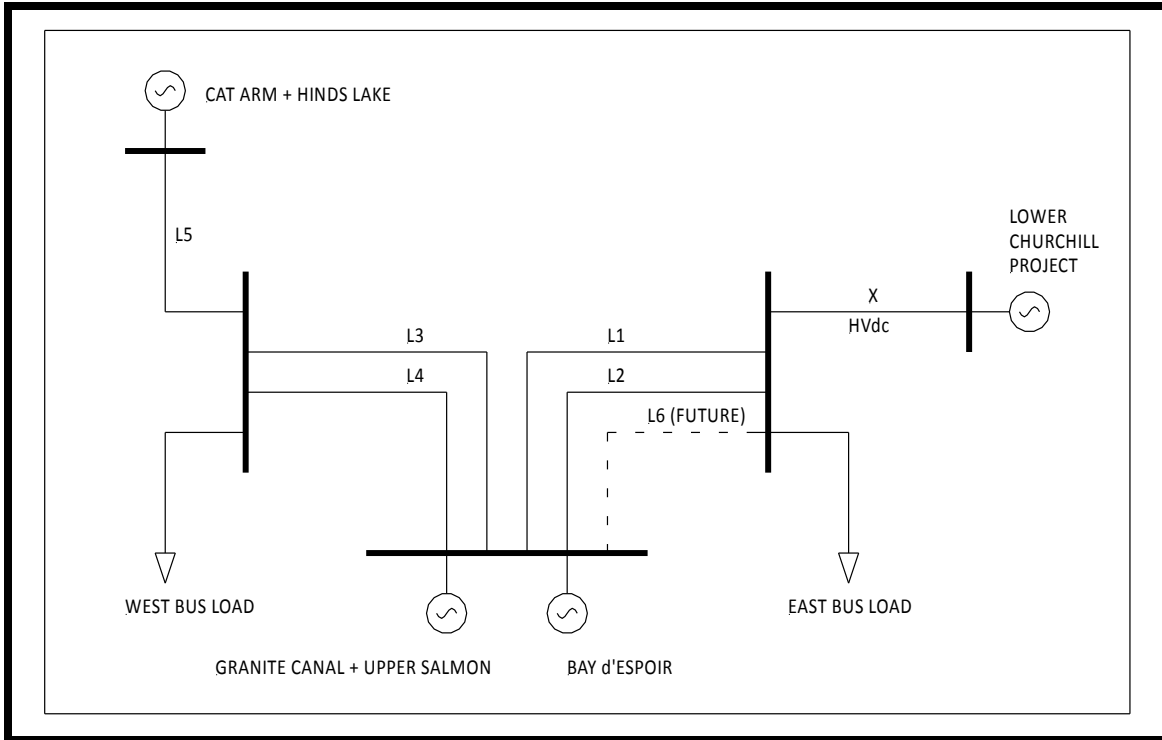


Figure 4.15 - Single Line Diagram of the Island's Bulk Electric Power System at 230 kV Level

4.3.1 Model Assumptions

The following assumptions are made in this study:

- The proposed HVdc tie line to Maritimes is excluded
- Both converter stations are available 100% of the time
- The submarine cable system is available fully
- The generation failure at the Gull Island plant is not included
- HVdc line capacity of 800 MW (approximately 750 MW delivered after losses) is treated as a source

- The bipole failure rate used in the analysis considers only the permanent faults due to wind and ice loads; temporary outage due to lightning is not considered.
- Island system load (NLH component) is matched only against the hydraulic generation (Thomas, 2009)
- A minimum of 3% margin is required to maintain the balance between system peak load and the installed capacity (hydraulic generation only)
- System analysis is based on annual hourly load variation rather than system peak load
- The failure rates are controlled through design return period values
- The repair rate variation indicates the severity and the extent of the HVdc line failure; for example 1 day repair may indicate a simple X-arm failure while a 7 day repair may indicate a small number of tower failures.
- System component failure modes are independent
- Common mode failure is not included
- The island transmission line system is modeled only at the 230 kV level
- Cat Arm plant is modeled as one unit with full capacity and Hinds Lake generation is assumed to be available 100%. 138kV line from Hinds Lake to Howley is not included
- System loads at east and west bus points are based on historical data (Thomas,2009)

- Component failure and repair rates are based on historical operational data
- HVdc line repair rates control the severity of line failure and the extent of the failure zone (to be discussed later)
- Common mode failure is not included for lines on the same corridor
- Gas turbine capacity as back up generation is included in the revised model only at the East Bus point
- HVdc line is assumed to be in service by 2016 and the Holyrood plant will be decommissioned in 2016
- All initial line costs are given in 2008 dollars and escalated to 2016 dollars using data provided by Paul Stratton from System Planning Department
- Total system state probabilities are calculated at least up to three 9 digits or greater (> 0.999)
- Future line L6 (Figure 4.15) is not included in the present model but can be added in the future

4.4 System Indices Evaluation - Equivalent Model

The bulk electric power system is quite complex and often consists of several generating plants interconnected to various substations for load distribution via a network of high voltage transmission lines. The actual modeling could be quite complex and often computationally intractable if one has to include all the bus points as well as

all voltage levels for the power system. Therefore, the adequacy equivalent approach proposed by Billinton et. al (1995) is used in this study.

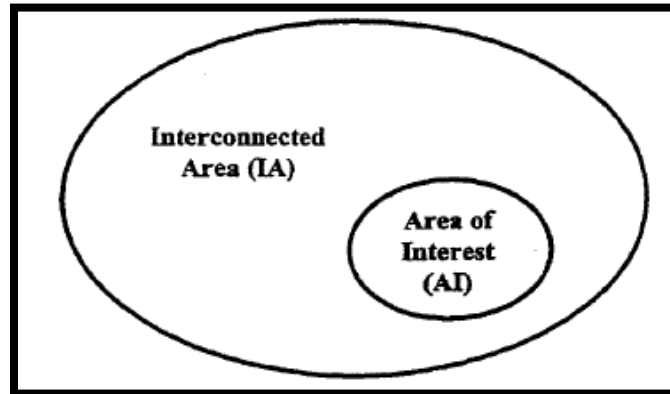


Figure 4.16 - Schematic Diagram for IA and AI

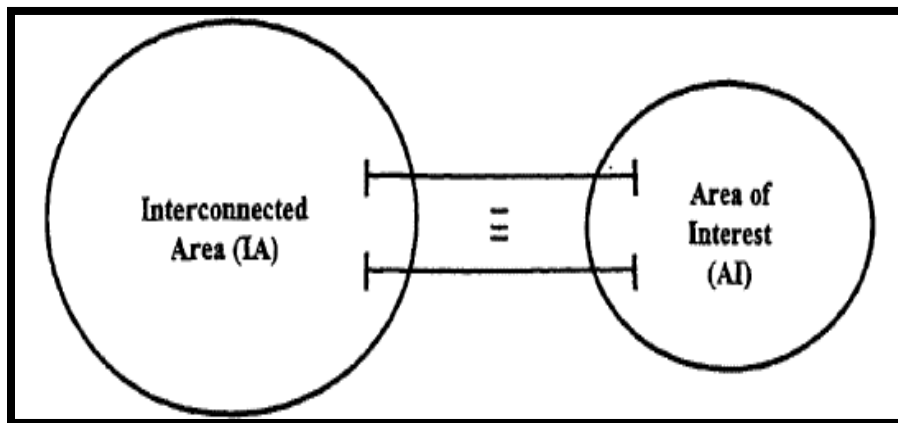


Figure 4.17 - Sketch Showing the IA and AI (Zhang, 1995)

The bulk system is divided into two areas, one being the interconnected area (IA) and the other being area of interest (AI). IA and AI can be connected via tie lines with some functional properties. Figure 4.16 presents the schematic of the concept.

The assumption in the analysis is that any excess power capacity from, the interconnected area (IA) can be transported to the area of interest (AI) via tie line(s). The indices are computed for the total system and can be broken down at bus points.

For detailed analysis of a complete system, a computer program has been developed in Excel spreadsheet format which provides the **BEPS** adequacy indices.

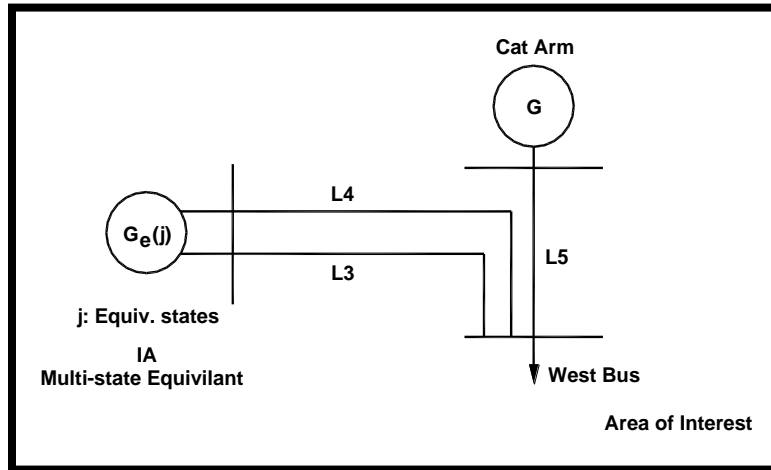


Figure 4.18 - Sketch Showing a Typical State Condition

If the total number of equivalent system states for IA is n_{eq} and the number of system states for AI is n_{ai} then the total system states will be $n_{ts} = n_{eq} * n_{ai}$. The severity of each system state is calculated and the adequacy indices for all the system states are summed up under a load step increment following the criteria described under Section 4.0 (Figure 4.11). The annual indices are calculated following equation 4.10. The input parameters are state probability, failure rate and the repair rate.

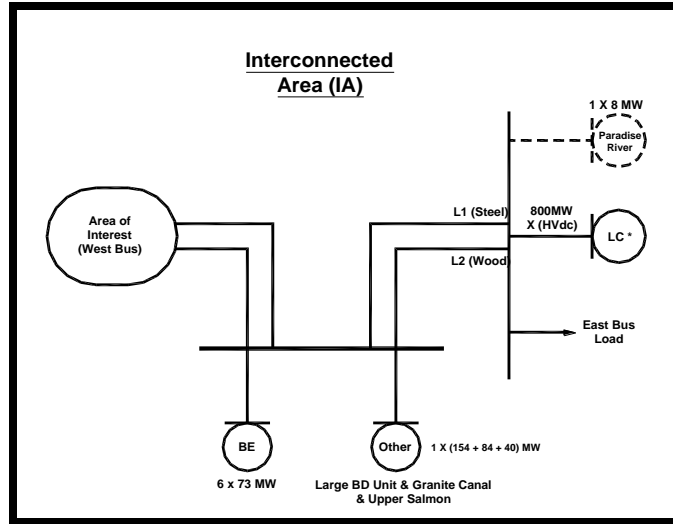


Figure 4.19 - Sketch Showing the Interconnected Area

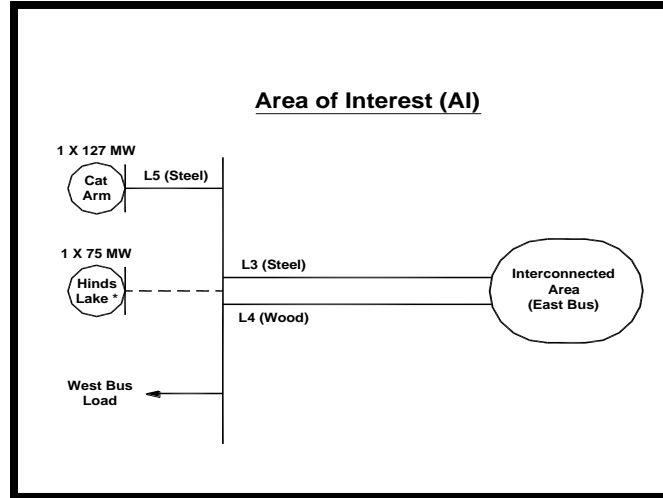


Figure 4.20 - Sketch Showing the Area of Interest

Given the importance of the HVdc Infeed system and its impact on the NLH system, the HVdc link (750 MW) in conjunction with other generation sources on the island (primarily hydraulic) is represented by a number of capacity states which consider the various component outages. Each state is represented by a state probability, frequency of occurrence of the state and the load curtailment if there is any. Once the **BEPS** indices are calculated for a specific year (say 2016), the **ECOST** is calculated following equation 4.16. This computation methodology will be described in Section 6.0.

5.0 Line Cost Model (LCOST)

In developing the line cost model, the line is treated as a system where the major components such as the tower, foundation, conductor, insulator and hardware are interconnected as a “link”. The structural design model considers this as a “series” system such that if one fails then the line fails and the bulk power supply is lost.

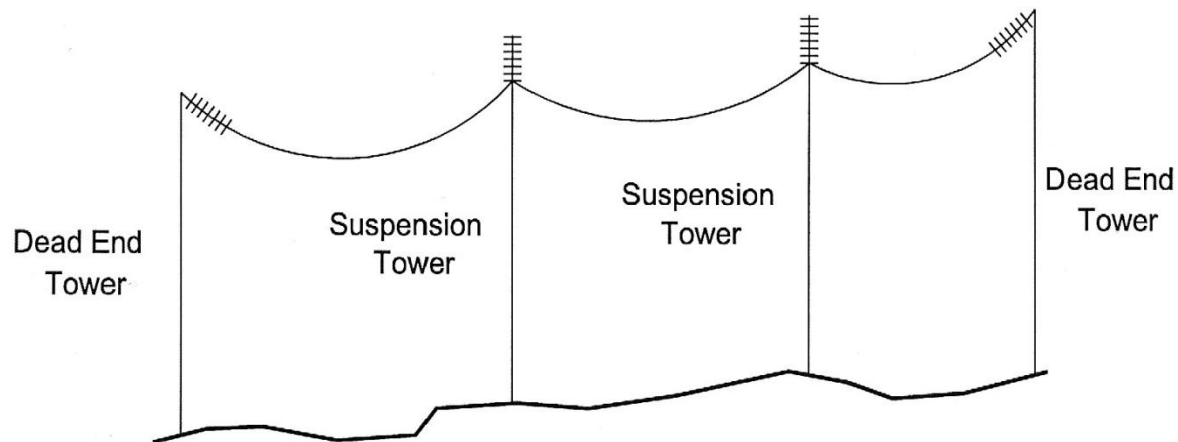


Figure 5.1 - Typical Line Layout

A line system consists of primarily three subsystems from mechanical strength point of view (Figure 5.2).

These are:

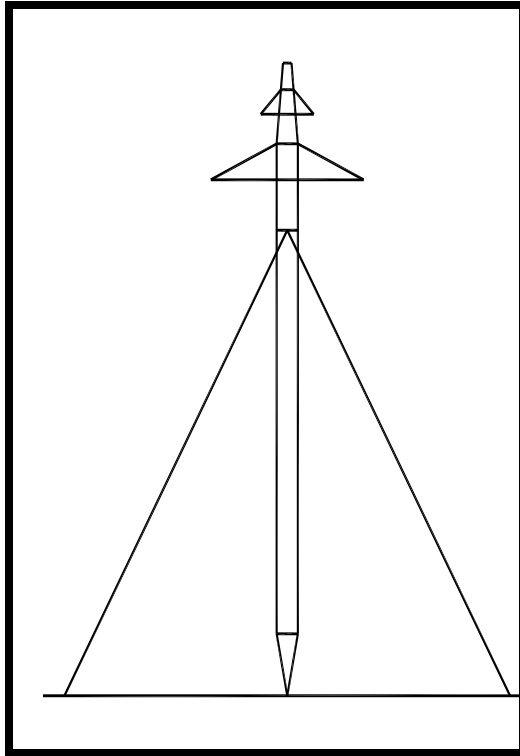
- (1) Suspension Tower Subsystem
- (2) Dead End Tower Subsystem
- (3) Conductor-Hardware Subsystem

Current philosophy in the design of a transmission line considers the line as being composed of various interactive elements and when loaded, failure of the weakest component results in the failure of the line. The reserve strength remaining in the other components does not have any effect on the failure load (limit load), but may influence

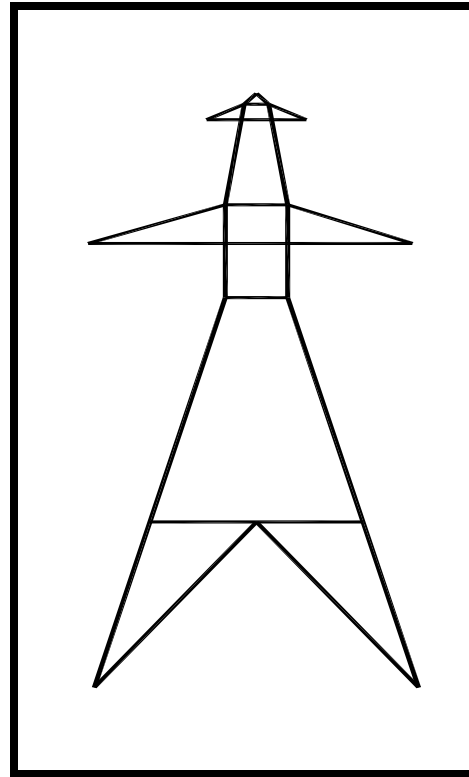
the secondary consequence of a failure. Based on a system approach where the strength of an individual component is properly coordinated with other components according to a preferred sequence of failure, it has been recommended in that the conductor element should be considered as the strongest element in the overhead line design (Haldar, 2006).

5.1 Framework for Developing Initial Line Cost

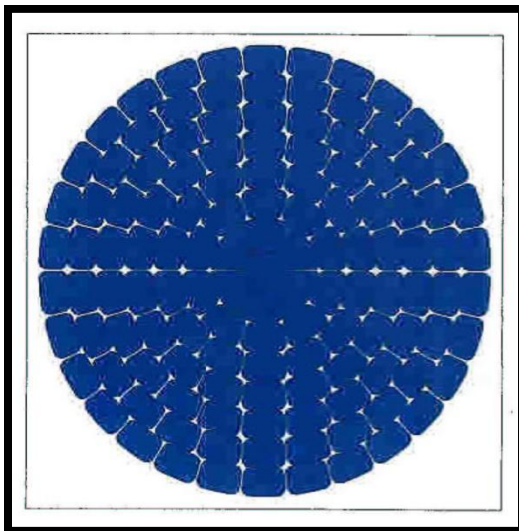
In developing the cost model, the material and installation costs of each major component of the line are considered explicitly. Figure 5.1 depicts a typical section of a line which consists of a number of tangent towers held by a fixed length of conductor supported at each end by two fixed dead end structures. The tangent tower could be self supported or guyed. Figure 5.2 presents some of the major components of the HVdc line system. This includes: (1) guyed tangent towers, (2) self supported heavy angle towers and dead end towers, (3) conductor and shield wires (4) insulators and (5) hardware arrangements on suspension and dead end towers.



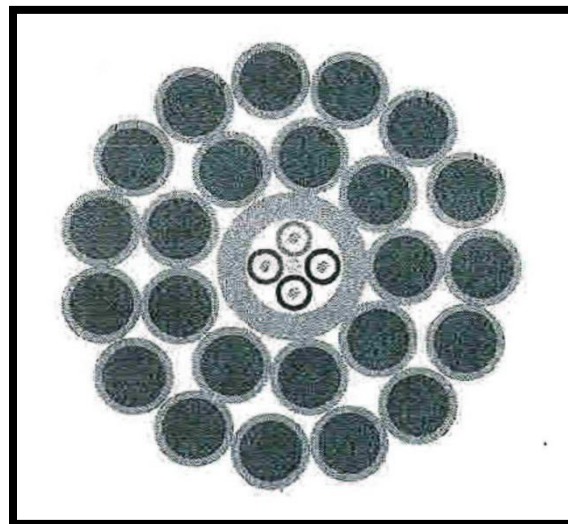
Suspension Tower



Strain Tower



Conductor Cross-section



Shield Wire Cross-section

Figure 5.2 - Typical Line Components

5.1.1 Environmental Line Loading

The HVdc line has been divided into three segments based on maximum expected environmental loading as follows **(Provided by John Walsh and K. Tucker, 2009)**:

- Segment 1: Normal Loading Section – 826 km
- Segment 2: Alpine Loading Section – 90 km
- Segment 3: Eastern Section – 176 km

Table 5.1 - Segment Maximum Ice Loading for Various Return Periods

Return Period of Loads	Segment 1	Segment 2	Segment 3
	Normal	Alpine	Eastern
50 years	47 mm	232 mm*	75 mm
150 years	56 mm	278 mm*	90 mm
500 year	66 mm	325 mm*	105 mm

Note: All Measurements shown above are radial ice thicknesses.

* Alpine loading segment values are calculated as a combination of glaze and rime and use an average ice density in the design.

Table 5.2 - Maximum Wind Loading for Various Return Periods

Return Period of Loads	Segment 1 and 3	Segment 2
	Normal and Eastern	Alpine
50 years	110 km/h	154 km/h
150 years	118 km/h	167 km/h
500 year	129 km/h	180 km/h

Note: The above wind speeds are constant wind speeds, not gust wind speeds. A gust factor is applied in the design to account for above normal gusts.

Table 5.3 - Combined Wind and Ice Loads

	RP	Max Ice and 35% Wind		Max Wind** (km/hr)	Combined	
		Ice (mm)	Wind (km/hr)		Wind (km/hr)	Ice (mm)
Section 1 Normal	50	47	38.5	110	55	23.5
	150	56	41	118	59	28
	500	66	45	128.5	64	33
Section 2 Alpine	50	232*	54	154	77	116
	150	278*	58.45	167	83.5	139
	500	325*	63	180	90	162.5
Section 3 Eastern	50	75	37.5	110	55	37.5
	150	90	41	118	59	45
	500	105	45	128.5	64	52.5

* Values shown are the sum of both glaze & rime ice with a 700 kg/m³ ice density used.

**Wind values shown are constant wind. Gust factors were applied during design.

5.2 Suspension (Tangent) Tower -Cost Model

A suspension tower is subjected to wind and ice loads, with these loads typically acting at the conductor and shield wire attachment points. **Figure 5.3** presents a typical loading diagram on a suspension tower. A detailed structural model was developed in the “**TOWER**” program (in-house program developed in mid 80’s) and a complete analysis/design check was made to ensure that all members under the design loads are within the safe stress level. The program provides the tower weight.

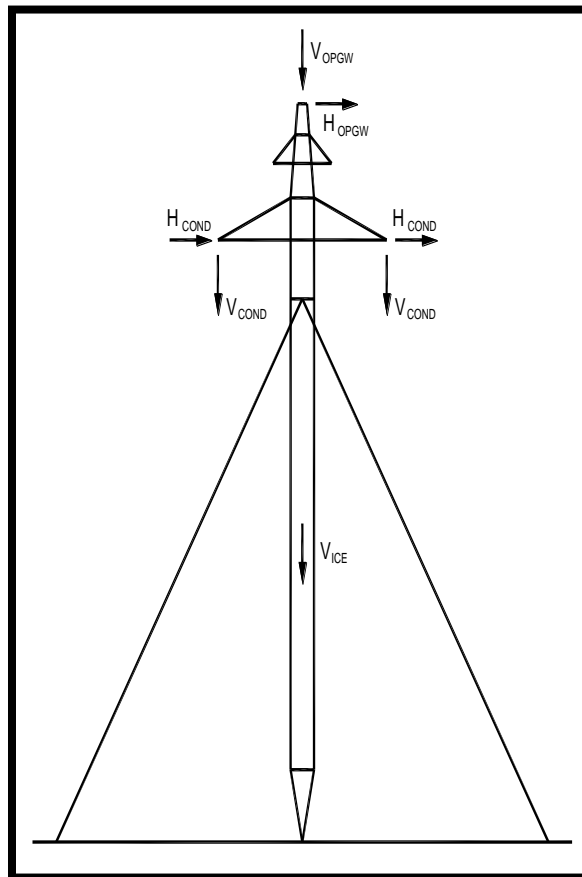


Figure 5.3 - Typical HVDC Suspension Tower

The tower weight, W , can also be estimated based on an empirical formula as

$$W = cKl(H^{0.65} + V^{0.5} + L^{0.5}) \quad [5.1]$$

where

c = empirical constant and is obtained from calibration (Redden, 2009)

K = a parameter determined from phase spacing

l = effective height where the resultant of all loads act

H = sum of all horizontal loads

V = Sum of all vertical loads including the ice weight on tower

L = sum of all longitudinal loads

The calibration constant, c is obtained from the weight estimated from the detailed “**TOWER**” model (Willette, 2009). Once the calibration constant is obtained, the weight for a similar group of towers can be easily obtained. **Table 5.4** presents the estimated tower-foundation weight and the cost for different line segments. The cost is determined as

$$CS_j = (W_j * \alpha_j) * factor \quad [5.2]$$

where

CS_j = unit cost of a suspension tower in segment j

W_j = weight of a suspension tower type in segment j.

α_j = unit cost of fabrication

factor = cost of erection

Table 5.4 - Suspension Tower Weights in Three Segments

	Segment 1	Segment 2	Segment 3
	Normal	Alpine	Eastern
Tangent Tower Weight (W_j)	5,650 kg	8,300 kg	5,300 kg
Tangent Tower Unit Cost (CS_j)	\$ 94,600	\$ 110,300	\$ 92,000

5.3 Strain (Dead End) Tower-Cost Model

A heavy angle dead end or a full tangent dead end tower is subjected not only to wind and ice loads on conductors, shield wires, etc. but also a vector component of the cable tension loads because of the line alignment. Figure 5.4 presents a typical loading diagram. A detailed structural model was developed in the “TOWER” program (Reddin, 2008) and a complete analysis/design check was made to ensure that all members are within the safe stress level. The program also provides the tower weight and an additional fixed weight for redundant members, plates and bolts included in estimating the total tower weight.

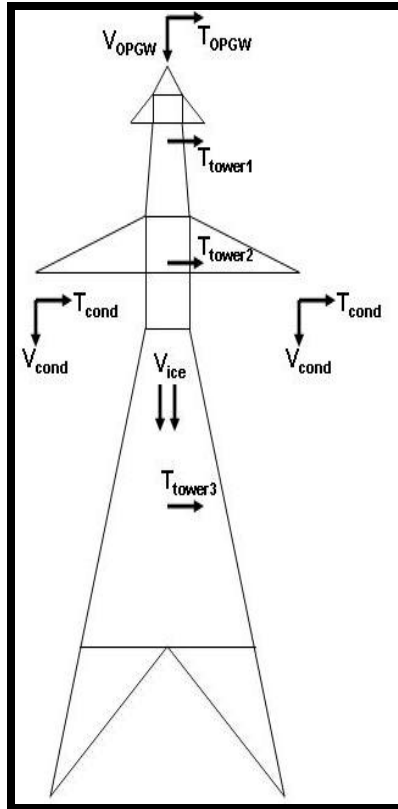


Figure 5.4 – Forces on a Typical Dead End Tower (Reddin, 2009)

The tower weight can also be estimated based on the formula in equation 5.4 the notation has been explained earlier

$$W = cKl(H^{0.65} + V^{0.5} + L^{0.5}) \quad [5.4]$$

The calibration was done and the final estimated weight for these angle dead end tower costs are given in Tables 5.5, 5.6 & 5.7.

Table 5.5 - Dead End Tower Weight & Cost

	Segment 1	Segment 2	Segment 3
	Normal	Alpine	Eastern
0-60 Tower Weight (W_{1j})	18,500 kg	23,500 kg	18,900 kg
0-60 Tower Cost (CD_{1j})	\$ 160,500	\$ 187,000	\$ 162,000

Table 5.6 - Dead End Tower Weight & Unit Cost

	Segment 1	Segment 2	Segment 3
	Normal	Alpine	Eastern
60-90 Tower Weight (W_{2j})	22,600 kg	28,200 kg	22,900 kg
60-90 Tower Cost (CD_{2j})	\$ 229,000	\$ 267,000	\$ 233,000

Table 5.7 - Dead End Tower Weight & Unit Cost

	Segment 1	Segment 2	Segment 3
	Normal	Alpine	Eastern
Anti-Cascade Weight (W_{3j})	23,700 kg	29,500 kg	24,100 kg
Anti-Cascade Cost (CD_{3j})	\$ 257,000	\$ 290,000	\$ 257,500

5.4 Conductor Cost Model

Table 5.8 presents the material and stringing costs of conductor and shield wires for the line segments. These costs are not dependent on the design return periods because the conductor size chosen remains constant for all three return period load levels

Table 5.8 - Conductor and Shield Wire–Material plus Installation Costs

Component	Segment 1	Segment 2	Segment 3	Total
	Normal	Alpine	Eastern	
Conductor	\$ 68.9 M	\$ 7.6 M	\$ 14.6 M	\$ 91.1 M
OPGW	\$ 18.9 M	\$ 2.1 M	\$ 4 M	\$ 25 M

5.5 LCOST Model (Equation 3.1 in Section 3.0)

Once the cost for each tower type (tower + foundation + insulator + hardware) in each segment is determined, the total line cost can be obtained as the sum of all tower-foundation cost for all tower types and the material and installation costs of conductor and shield wire.

The cost of all tower types including the foundations and the conductor for the entire line system is expressed in the following form

$$C_I = \sum_{i=1}^{Nseg} (ns_i CS_i + \sum_{j=1}^m nd_{ij} CD_{ij}) + \text{Cost of Conductor and Shield Wire} \quad [5.5]$$

where

C_I = initial cost of the line

ns_i = number of suspension towers in segment, i

CS_i = unit cost of suspension tower in segment, i

nd_{ij} = number of strain tower type, j in segment, i

CD_{ij} = unit cost of strain tower type, j in segment, i

$Nseg$ = total of number of segments representing the line

m = number of strain towers in segment, i

For suspension structures, ns_i are computed based on the typical design span and the segment length. The unit tower cost also includes foundation and insulator and hardware cost for each tower type. Table 5.9 summarizes the cost of all tower types and Table 5.10 presents the number of each tower type in three line segments.

Table 5.9 - 50-Year Tower Unit Costs (CS_i & CD_{ij})

	Segment 1	Segment 2	Segment 3
	Normal	Alpine	Eastern
Tangent Tower Unit Cost (CS_j)	\$ 94,000	\$ 110,300	\$ 92,000
0-60 Tower Cost (CD_{1j})	\$ 156,500	\$ 186,000	\$ 158,000
60-90 Tower Cost (CD_{2j})	\$ 231,500	\$ 267,000	\$ 233,000
Anti-Cascade Cost (CD_{3j})	\$ 251,000	\$ 290,000	\$ 252,500

Table 5.10 - 50-year Tower Quantity Matrix for Various Line Segments (ns_i & nd_{ij})

	Segment 1	Segment 2	Segment 3
	Normal	Alpine	Eastern
Tangent Tower	1769	378	440
0-60° Strain Tower	55	12	29
60°-90° Strain Tower	6	6	2
Anti-Cascade	96	32	24

Similar calculations were carried out for 150-year and 500-year design loads and the tower weights and costs were determined. Equation 5.5 was used to derive the line costs for various return periods. The line costs with return periods in Table 5.11 are in 2008\$. Later in Section 7.0 these costs are escalated to 2016 dollars using standard escalation data provided by Paul Stratton from the System Planning Department (2009).

Table 5.11 - Total Cost for Selected Return Periods (2008\$)

Return Period	Segment 1	Segment 2	Segment 3	Total
	Normal	Alpine	Eastern	
50 yr	\$ 288 M	\$ 64.7 M	\$ 68.6 M	\$ 421.3 M
150 yr	\$ 293 M	\$ 89.7 M	\$ 78.6 M	\$ 461.3 M
500 yr	\$ 318 M	\$ 114.7 M	\$ 83.6 M	\$ 516.3 M

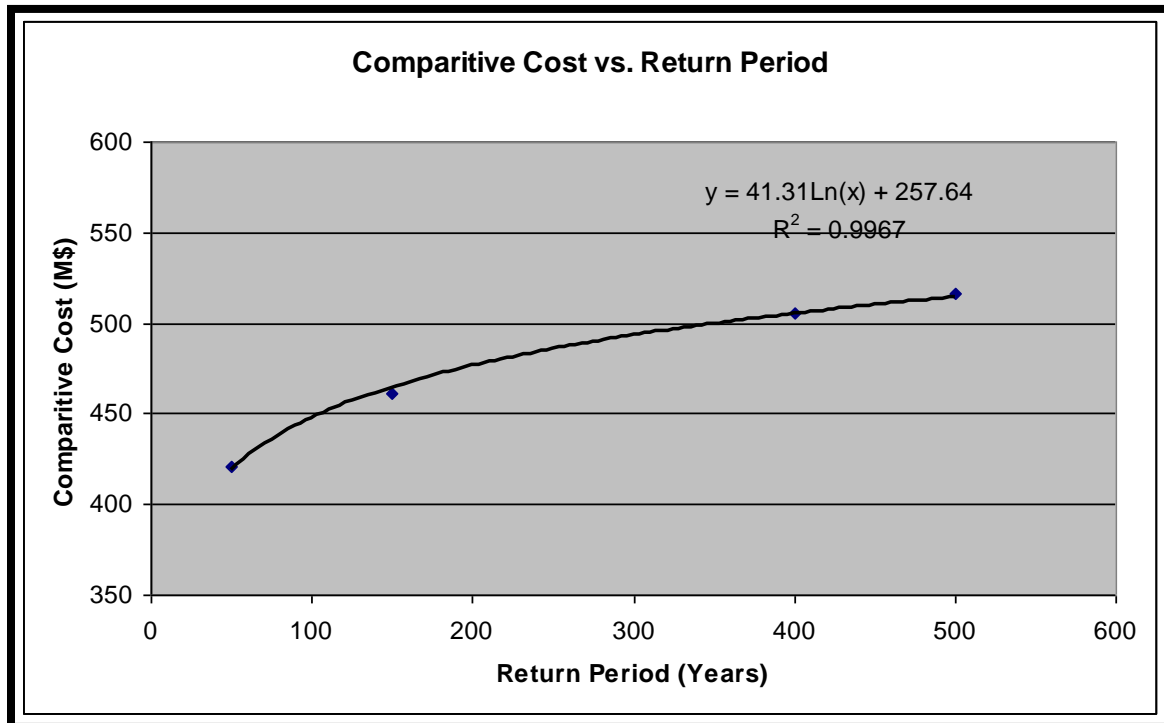


Figure 5.5 - Initial Line Costs with Respect to Various Design Return Periods

The line cost for a 400-year return period design load was also carried out independently using the **LCOST software** and was calculated to equal \$505.1M. Based on the regression analysis of three data points presented in Figure 5.5, the predicted line cost value for a 400-year return period compares well with the computed value. This confirms that the regression curve follows a reasonable trend line.

6.0 ECOST Model (Equation 3.1 in Section 3.0)

A brief review of literature indicates that there are three methods that can be used in developing such a cost model. In the first approach, the unit unsupplied energy cost can be estimated based on the ratio of gross domestic product (GDP) and the total electrical consumption. In this approach typically the cost is always underestimated and does not reflect the true value of the customer interruption (damage) cost.

In the second case, the analysis considers the actual “**black out cost**” after it has happened. For example, some investigators (Billinton et al, CIGRE 2001) have used the New York City blackout in 1976 to assess the actual interruption cost. In the study, both tangible and intangible costs are included in deriving the customer damage cost. Post disturbances cost data after significant power disturbances in Australia, New Zealand, Canada, Norway, Sweden and the United States are summarized in the CIGRE report.

The third approach primarily developed by **Professor Roy Billinton and his associates** over the past three decades use the customer survey data where the outage cost is assessed based on monetary costs/losses due to unavailability of power supply for various durations and frequencies. CEA initiated a major R & D project in 1979 (Billinton et. al, 1982) where the questionnaire was carefully developed to get the necessary cost information for various customer groups (residential, commercial and industrial). A total of 15,000 questionnaires were sent nationwide and 5,000 responded. There were 475 responses from Newfoundland and Labrador. Direct costs are relatively easy for commercial and industrial customers but are less tangible for residential customers. According to Billinton, “A major advantage of the survey method is that it can be tailored to obtain the specific information which is important to the utility industry”. The survey data is grouped appropriately by sector. A typical database on the Customer Damage Function (CDF) is presented in Table 6.1. The utility can develop its own database following the methodology outlined in the CEA report.

Table 6.1 - Customer Interruption Data (Base Case, 1991 \$/KW, Billinton, 2008)

User Sector	Interruption Duration				
	1 min	20 min	1 hr	4 hr	8 hr
Industrial	1.625	3.868	9.085	25.163	55.808
Commercial	0.381	2.969	8.552	31.317	83.008
Residential	0.001	0.093	0.482	4.914	15.690

The sector based interruption cost data (**CDF**, \$/KW) can be grouped together at a particular load point to provide an aggregated cost data often called Composite Customer Damage Function (**CCDF**). The assumption is that all load curtailment will be distributed proportionally at a load point according to customer distribution shown in Figure 6.1 and in Table 6.2

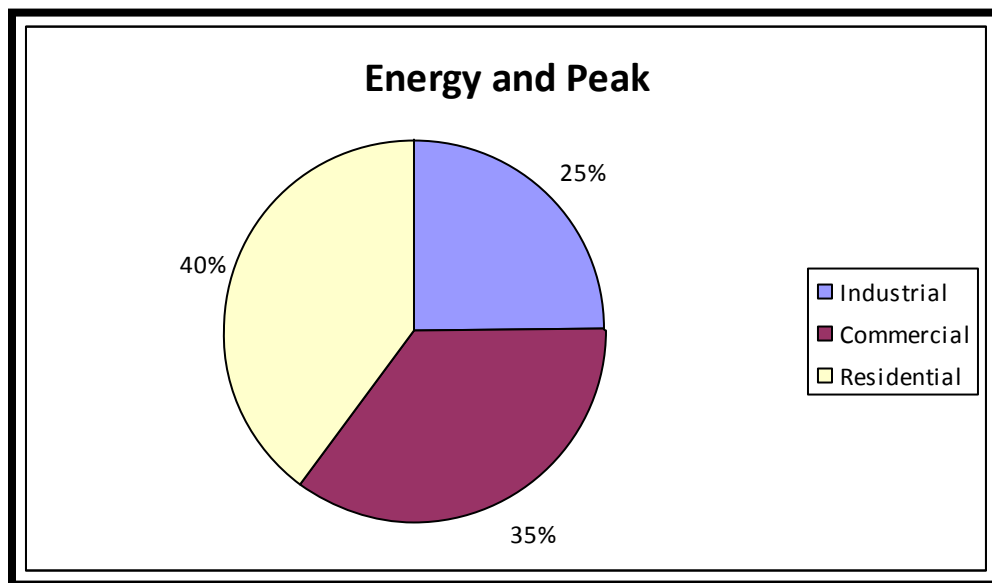


Figure 6.1 - Customer Distribution

Based on the sector distribution of customers presented in Figure 6.1, the typical unit cost for **CCDF** (\$/kWh) can be estimated using a weighted approach in Table 6.2. Figure 6.1 presents the **CDF** (\$/KW) for three different customer groups and the aggregated values. Figure 6.2 presents the **CCDF** values (\$/kWh) graphically.

Table 6.2 – CCDF (1991\$*)

User Sector	Interruption Duration				
	1 min	20 min	1 hr	4 hr	8 hr
Industrial	1.625	3.868	9.085	25.163	55.808
Commercial	0.381	2.969	8.552	31.317	83.008
Residential	0.001	0.093	0.482	4.914	15.690
Composite Customer Damage Functions					
CCDF \$/kW	0.540	2.043	5.458	19.217	49.281
CCDF \$/kWh	32.40	6.129	5.458	4.804	6.160

* These values have been escalated to 2016 \$ in Section 7.0 in the analysis

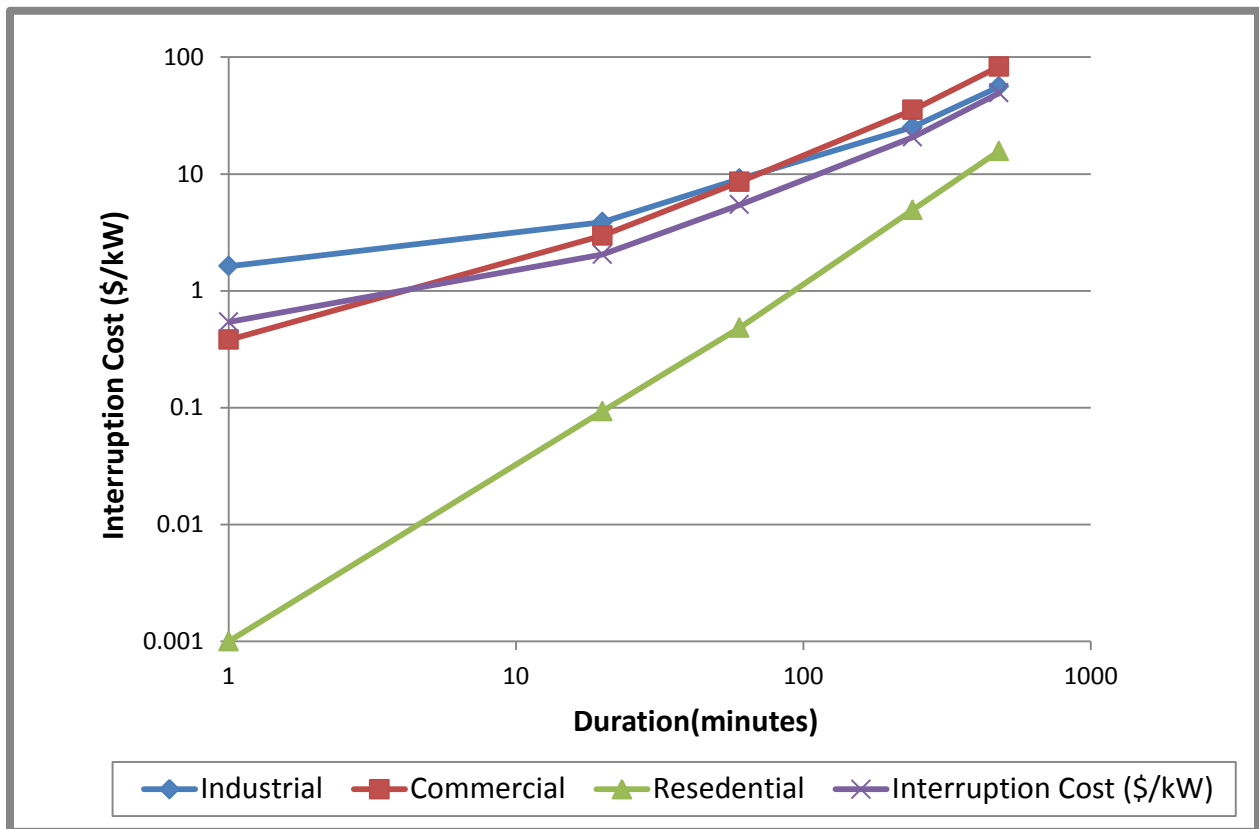


Figure 6.2 - Customer Damage Function (Billinton, 2008-CEATI Project 3347)

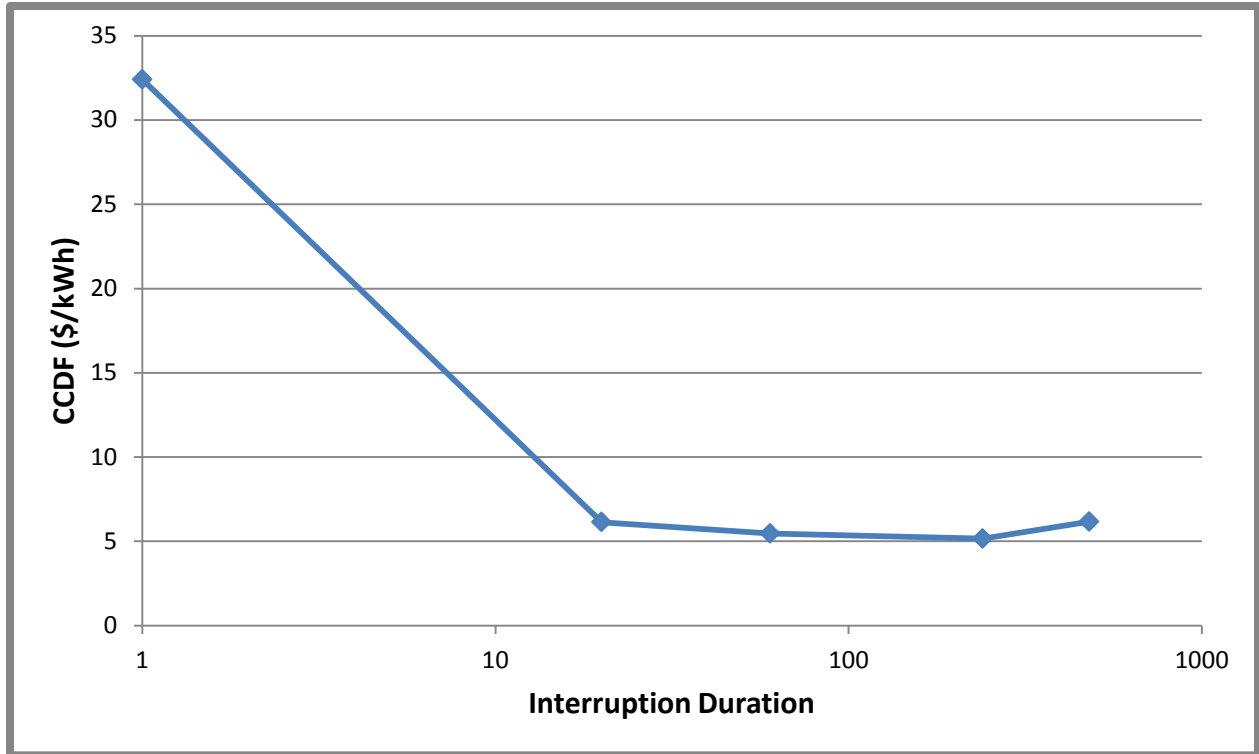


Figure 6.3 - Composite Customer Damage Function (CCDF)

The expected customer interruption cost (**ECOST**) is related to expected energy not supplied (**EENS**) in equation 6.1.

$$\mathbf{ECOST} = \mathbf{IEAR} * \mathbf{EENS} \quad [6.1]$$

where **IEAR**= Average Interrupted Energy Assessment Rate

The expected cost **ECOST** can be determined explicitly as

$$\mathbf{ECOST} = \sum_1^n L_i c(d_i) f_i \quad [6.2]$$

where

L_i = load curtailment at a i^{th} state,

$c(d_i)$ = customer damage function interpolated or extrapolated from Table 6.2 for a specific duration d_i

f_i = frequency of interruption (load curtailment)

If the duration in hours is outside the value given in Table 6.2 it is extrapolated linearly. Once the annual energy cost is determined this can be added to the expected cost of failure, C_f which is determined based on the replacement cost of the failed line section,

C_R

$$C_f = p_f * C_R \quad [6.3]$$

where p_f is the probability of line failure and C_f is the cost of failure. The present value of the customer damage cost and the cost of replacement of the line is calculated as

$$NPV = \sum_{i=0}^n \frac{\gamma_i (ECOST + C_f)_i}{(1+r)^i} \quad [6.4]$$

where

n = service life or the planning horizon

r = discount rate

γ_i = escalation factor in year, i

This cost should be added to the initial line cost of various return periods (**LCOST**) to obtain the total cost given in equation 3.1 and shown in Figure 3.1.

7.0 Results (Base Model without GT)

In assessing the HVdc line failure cost and its impact on the NLH system at the 230 kV level, a base model is considered first (Figure 4.15). The base line failure rate, λ for the HVdc line is considered as 0.02 occurrence/year (50-year return period). Similarly, the repair rate, μ (occurrence/year), is considered as 52.2 (moderate damage, seven day repair time).

All 230 kV steel lines on the island are assumed to have a failure rate of $\lambda=0.02$ while the wood pole line system is assumed to have a failure rate of $\lambda=0.2$. The high failure rate for the wood pole line system is chosen based on the wood pole line condition assessment under the Wood Pole Line Management Program (Haldar, 2004)

The failure rate and the repair rate data for all generating units (hydraulic units) are derived from the actual operating data collected over a 10-year period and the calculation was done following CEA guidelines on reporting outage data (CEA outage report). The numbers used in this study have been confirmed by the System Planning Department and the System Operations group.

For the economic analysis, the base discount rate is set at 8% (Stratton, 2009). The transfer capacity (MW) of each 230 kV line used in the analysis is provided by System Planning Department (Thomas, 2009). The System Planning Department also provided the long term load forecast data on the island. Based on the current installed capacity (hydraulic plants), it was estimated that load forecast at year 2031 will only provide a 3% margin. Based on the assumption described in Section 4.2.2, two planning horizons are considered in the sensitivity study. These are: 15 years and 50 years respectively.

7.1 System SI for Base Model ($\lambda = 0.02$, $\mu = 52$)

Figure 7.1 presents the system severity index (minutes/year) for a 50-year return period and seven day repair time for the HVdc line at the 2016 system load level.

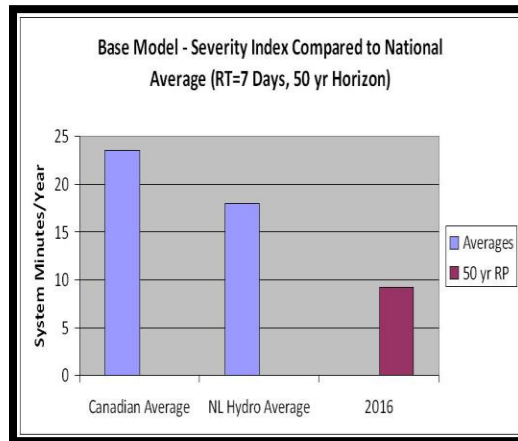


Figure 7.1 - Comparison of Severity Index (RP=50 years, MTTR=7 days)

It appears that the typical “blackout time” under this scenario is well below the national and NLH average as reported in CEA outage study report (2005). Figure 7.2 presents the severity index values for system loads at 2016 and 2031 levels (seven day repair time). The plots clearly show that the system “blackout” time at the 2031 load level will not exceed the reported CEA average outage time but will exceed the Hydro average outage time.

7.2 Sensitivity Study

Table 7.1 provides the parameters to be included in the sensitivity analysis. Table 7.2 presents the typical sector distribution based on 2016 system loads. The **IEAR** base case is calculated using the data in Table 6.2 escalated to 2016 level and the sector data presented in Table 7.2.

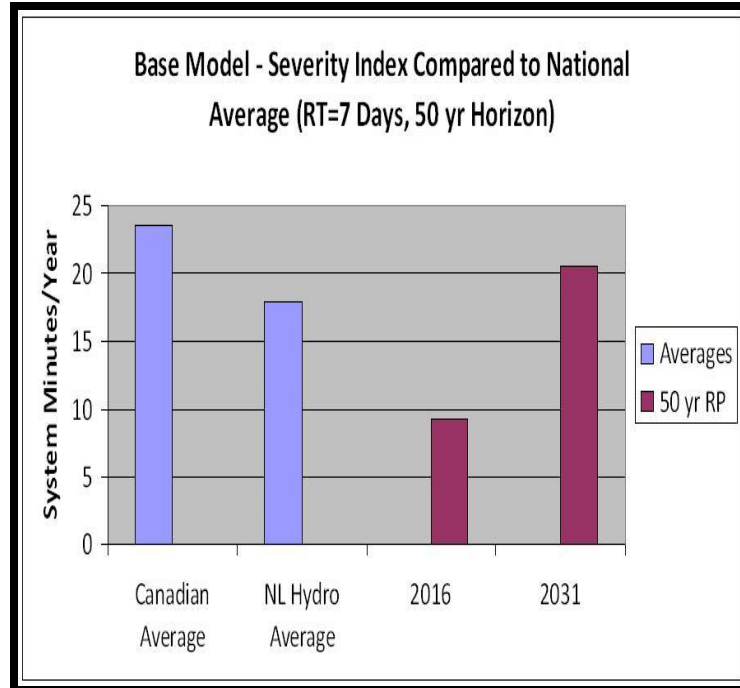


Figure 7.2 - Comparison of Severity Index (RP=50 years, MTTR=7 days)

Table 7.1 - Sensitivity Study-Parameters

Parameters	Base Case	Ranges	Units	Remarks
λ	0.02	0.002-0.02	failure occurrences/year	Frequencies
μ	52	1-20	repair occurrences/year	Severity of the failure
Planning Horizon	50	15 & 50	years	Service Life
IEAR	Billinton (2009)	Base rate halved & doubled	\$/kWh	Composite Customer Damage Function
Discount rate	8	6-10	percentage	Interest rate
C_R	2.0	2-10	million dollars	Replacement cost of the failed line

Table 7.2 - Sensitivity Study-Parameters

	Expected System Load in 2016			
	East		West	
	Load	%	Load	%
Residential	637	0.620918	313	0.649541
Commercial	286	0.278963	141	0.291823
Industrial	103	0.100118	28	0.058637

7.2.1 Line Failure Rate (λ)

Figure 7.3 presents the sensitivity of severity index (SI) with respect to variation of line failure rates. The data is presented for 2016 and 2031 system loads and for three return period values. A 500-year return period design option reduces the SI value significantly compared to a 50-year return period design.

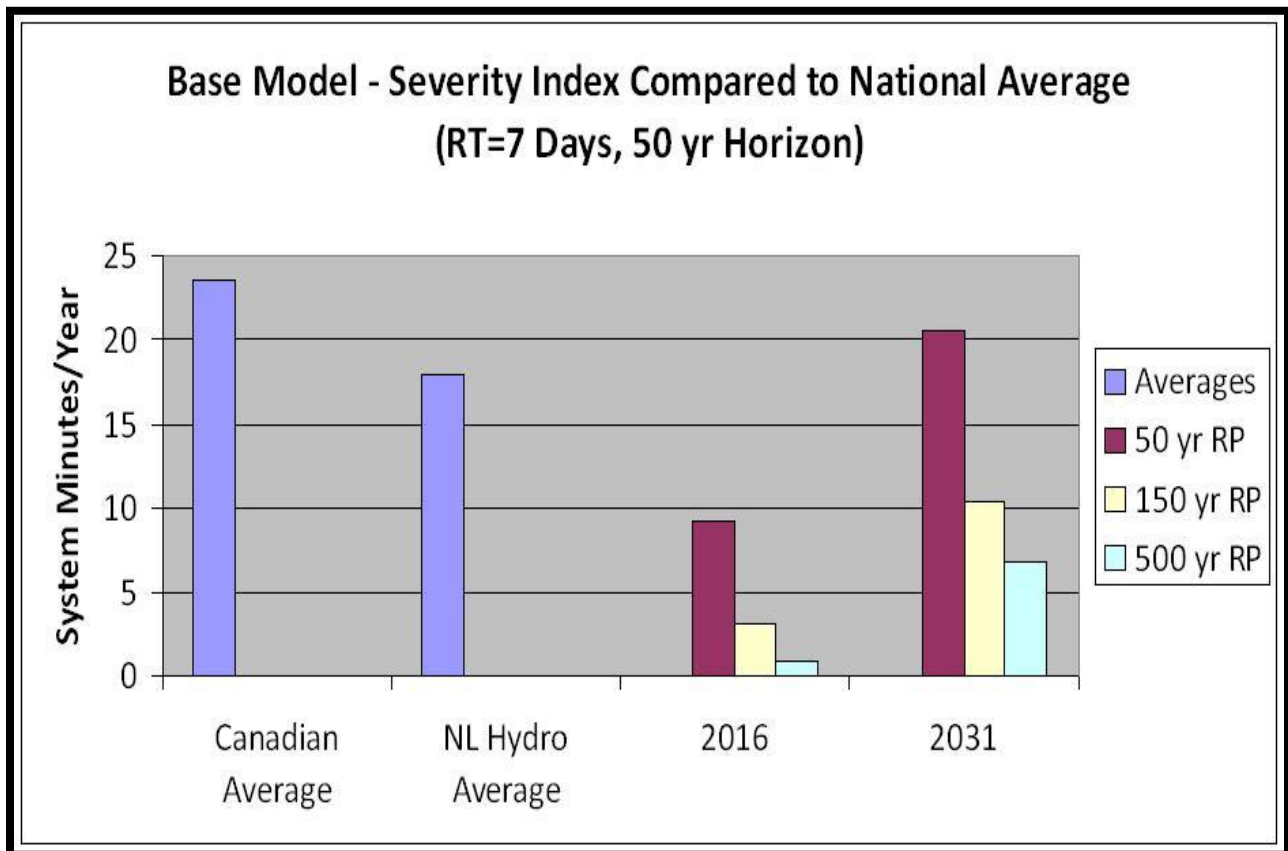


Figure 7.3 - Comparison of Severity Index for Various Return Periods

7.2.2 HVdc Line Repair Rate (μ)

Figures 7.4A and 7.4B present the sensitivity of the SI values with respect to variation in HVdc line repair rates (repair times). A one day line repair time implies a repair rate of 365 occurrences per year. The data is presented for 2016 and 2031 system loads. For the 2031 load level, the SI value for a 50-year design return period is twice that of the Canadian average (Figure 7.4b) when the repair time is 20 days (18.25 occurrences per year). However, this SI value reduces significantly if the design return period is 500 years.

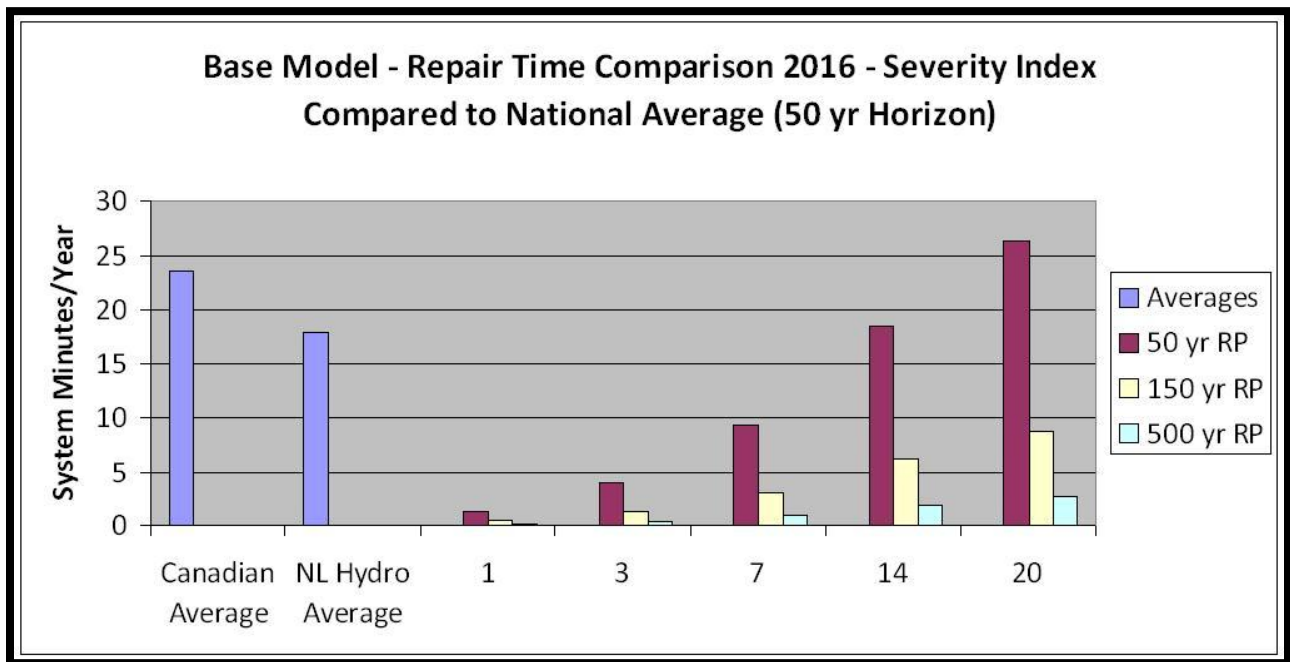


Figure 7.4a - Comparison of Severity Index for Various Repair Rates

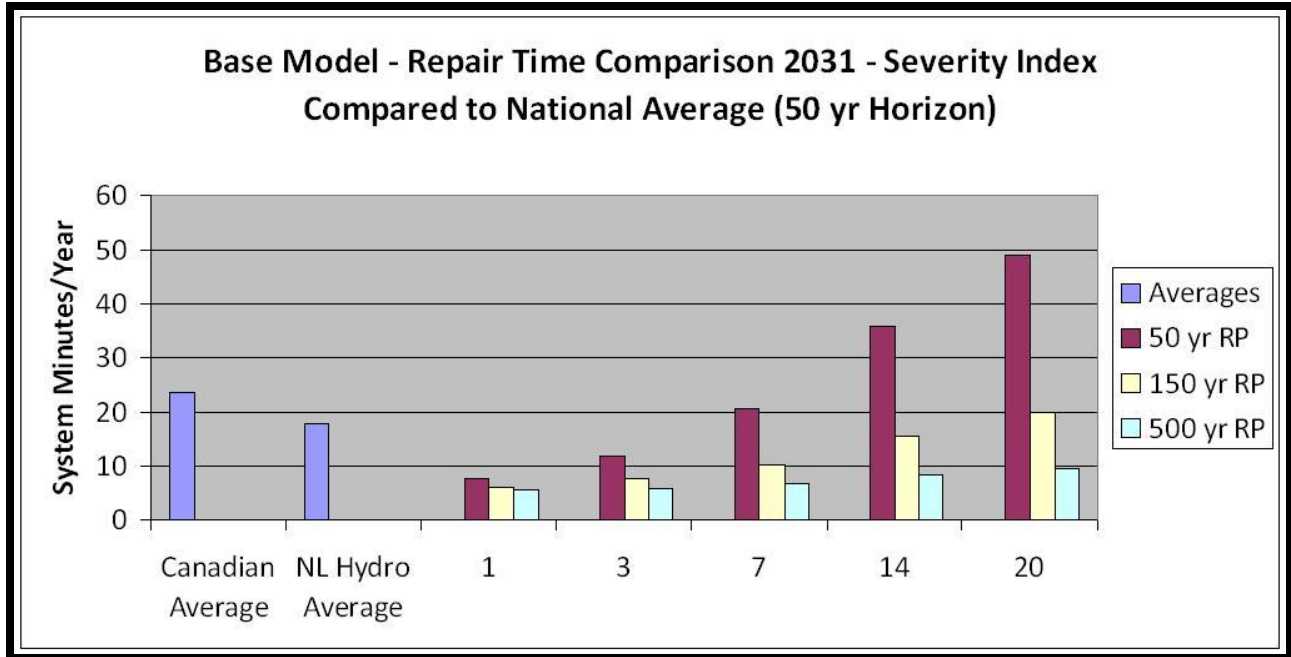


Figure 7.4b - Comparison of Severity Index for Various Repair Rates

7.2.3 Planning Horizon (15 years versus 50 years)

Figure 7.5 compares the present value of the unsupplied energy cost (**ECOST**) for two planning horizons. The data is presented for 2016 and 2031 system loads. All other parameters are chosen from the base case scenario. It is shown that the **ECOST** for 50-year planning horizon is approximately 2.5 times the cost of unsupplied energy considering a 15-year planning horizon. For this study, we will use a 50-year planning horizon.

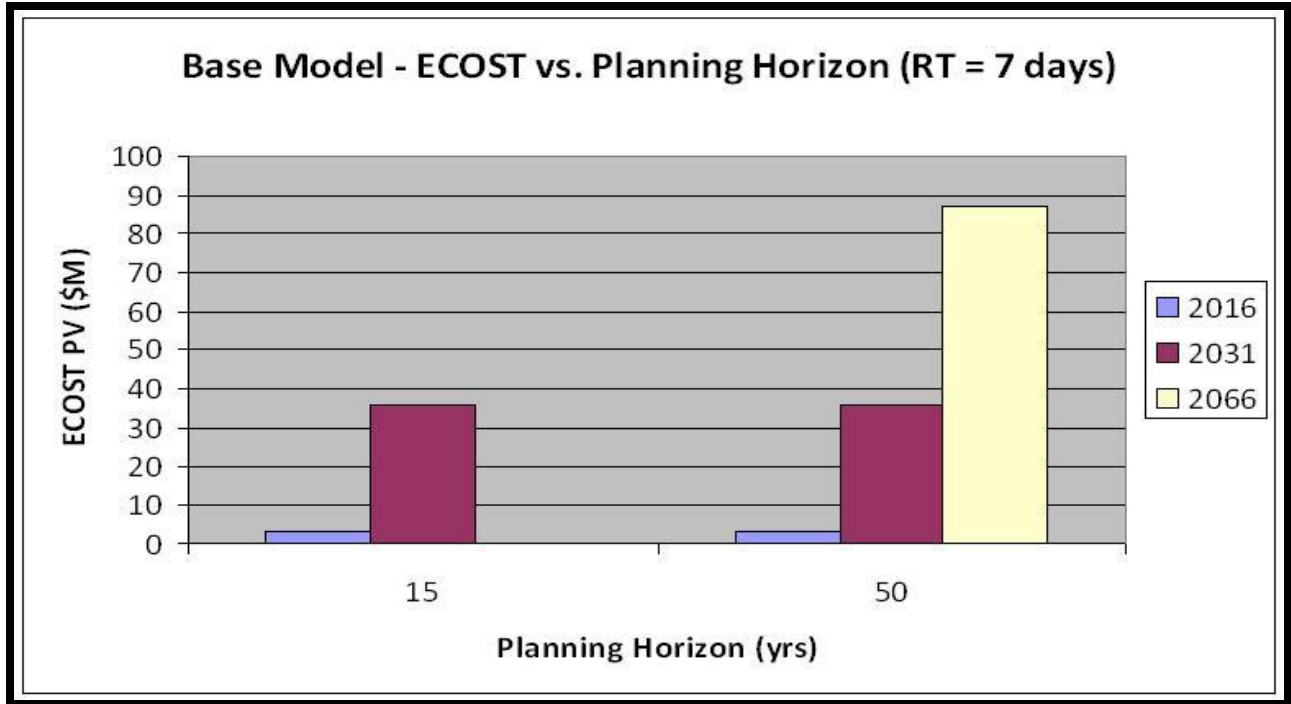


Figure 7.5 - Comparison of Present Values of Unsupplied Energy Cost

7.2.4 IEAR parameter

Figure 7.6 compares the **ECOST** values with respect to sensitivity of **IEAR** values. The data is presented for 2016 and 2031 system loads. “B” represents the baseline **IEAR** computed in Table 6.2 following Billinton (2009) and the two other values presented are adjusting the baseline values to 50% and 200% levels. It shows a linear trend in **ECOST** versus **IEAR** values for 2031 system loads.

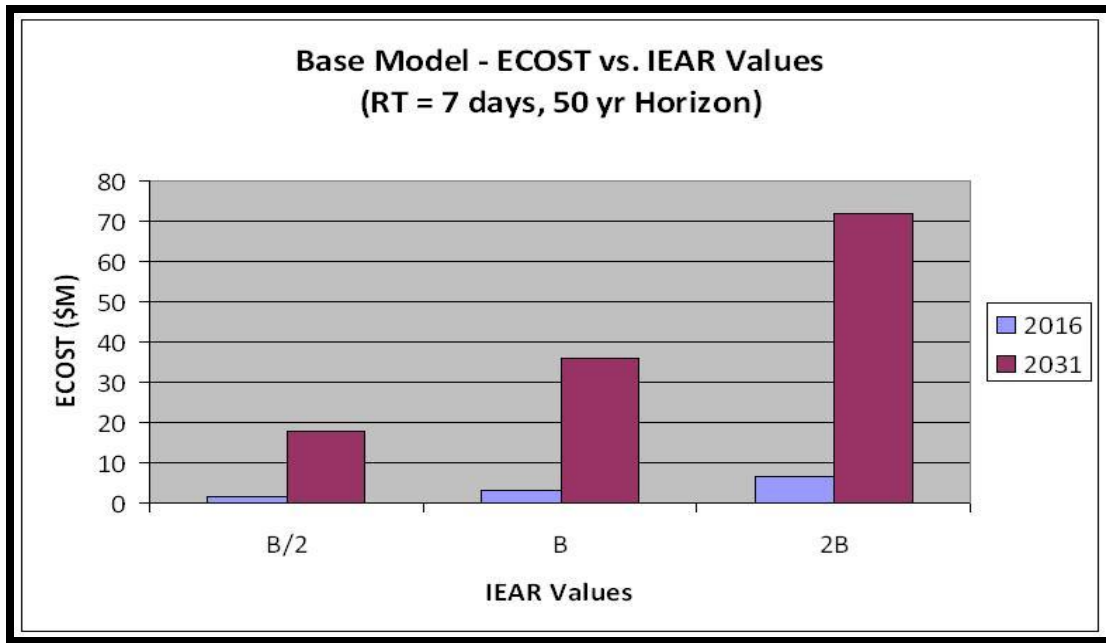


Figure 7.6 - Sensitivity of Present Values of Unsupplied Energy Costs

7.2.4.1 Discount Rates

Figure 7.7 compares the sensitivity of the annual **ECOST** value with respect to discount rate. The data is presented for 2016 and 2031 system loads. The present value decreases as the discount rate is increased.

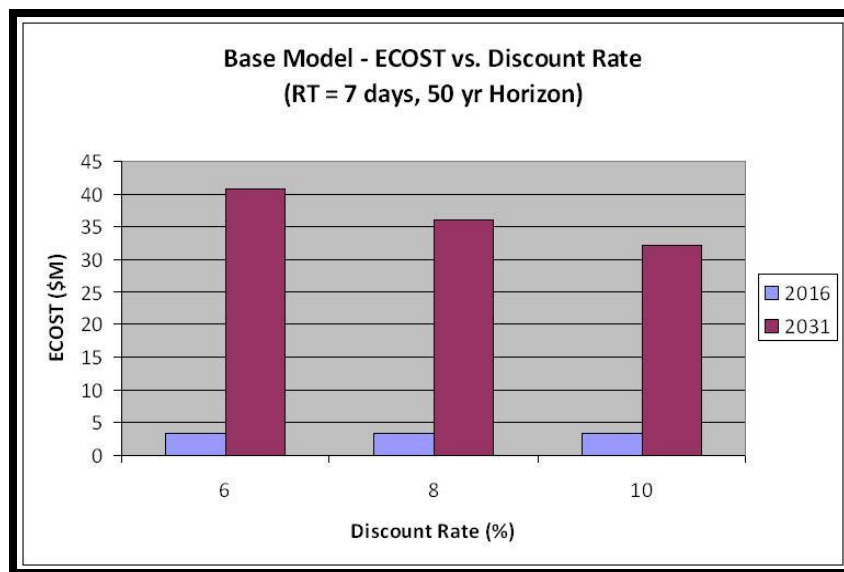


Figure 7.7 - Sensitivity of Present Values of Unsupplied Energy Costs

7.2.5 Cost of Line Replacement (C_R)

Figure 7.8 compares the sensitivity of the present value of the cost of failure (equation 3.1) with respect to line replacement cost. The data is presented for 2016 and 2031 system loads. The present value increases as the cost of line replacement also increase.

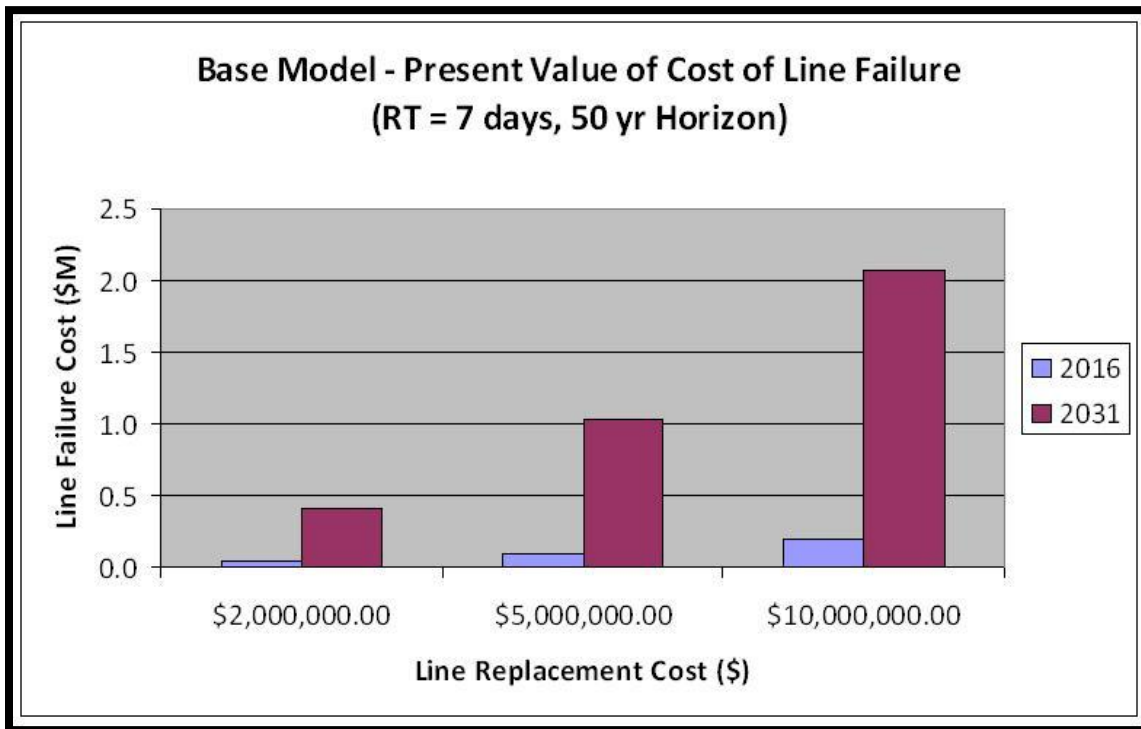


Figure 7.8 – Sensitivity of Present Values of C_f

7.3 Cost Optimization (15 years & 50 Years)

Figures 7.9 present the optimum cost versus return period for the base case. Figures 7.10 present the same for a 20-day repair time. It is clear from Figure 7.10 that for a repair time of 20 days (extended failure of HVdc line), it would be optimum to design the line for a return period of 150-year return period. The SI value will be slightly higher than the current NLH value reported.

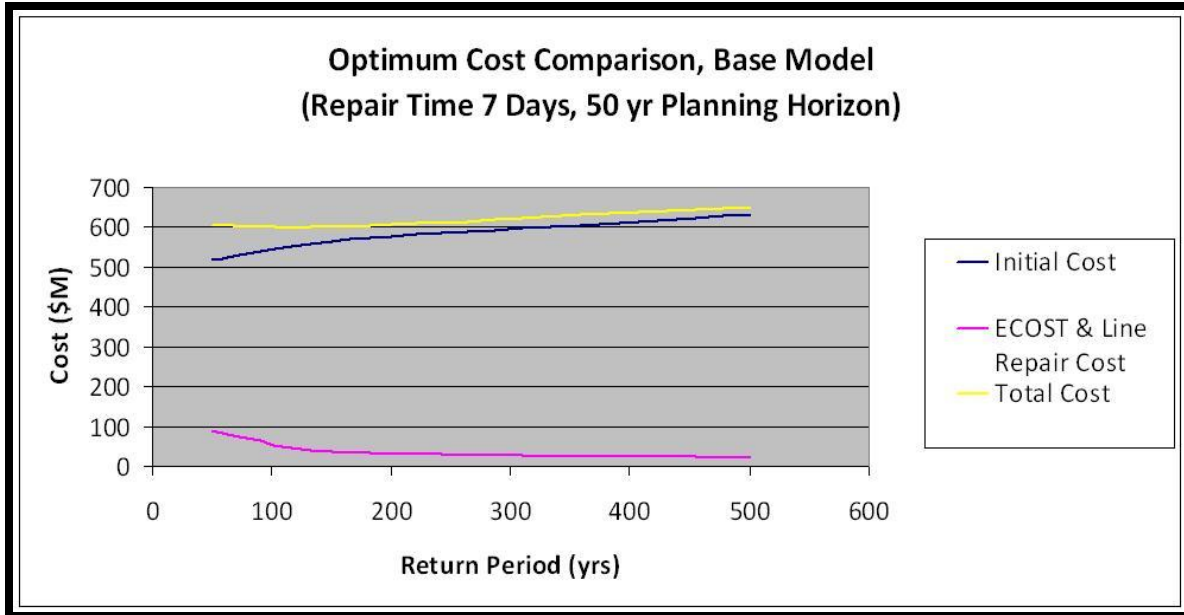


Figure 7.9 - Cost–Risk Plot for Various Return Periods

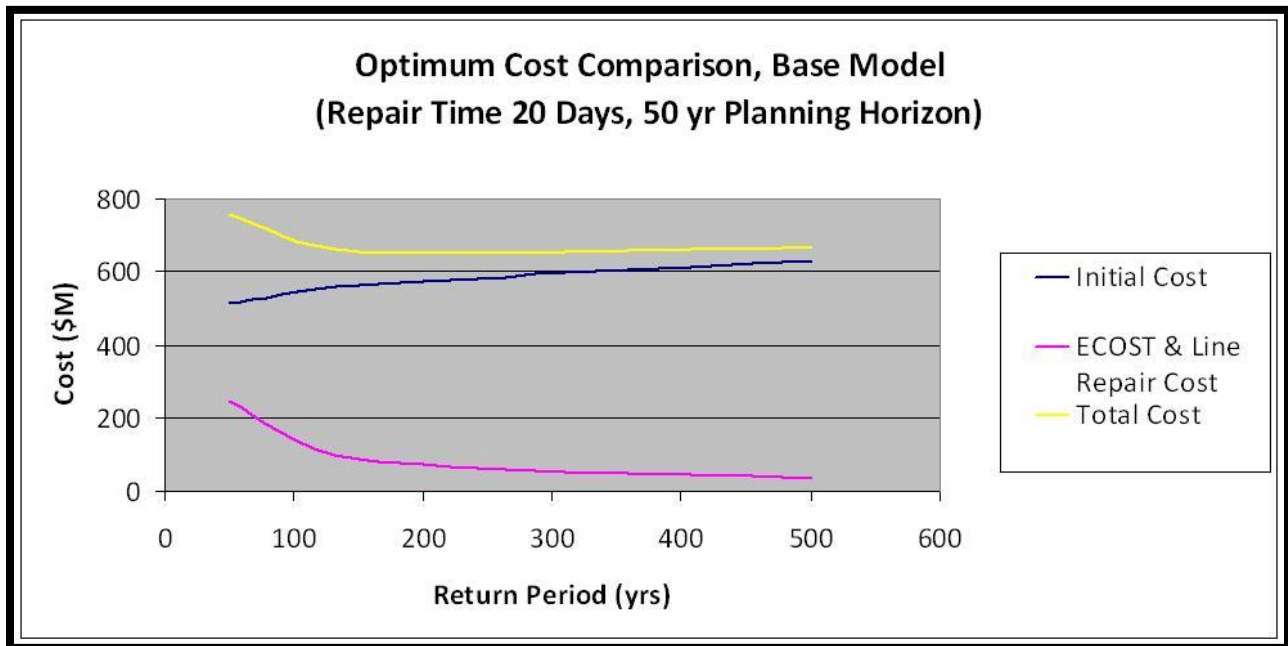


Figure 7.10 - Cost–Risk Plot for Various Return Periods

7.4 Benefit Cost Ratio (BCR) Analysis

The cost benefit analysis is done based on the net present value of the investment cost over a fixed planning horizon (50 years) and balancing this cost against the **NPV** of the future failure cost (**ECOST** plus the expected line failure cost, C_f).

Obviously the **BCR** needs to be greater than 1.0 in order to justify a specific design option with a return period value. The cost benefit ratio study shows that both design return periods 150-years and 500-years can be easily justified compared to 50-year design for a repair time of 20 days. In both cases, **BCR** is greater than 1.0. However for a 500-year return period design, the severity index is also reduced significantly and well below the national average value (Figure 7.3).

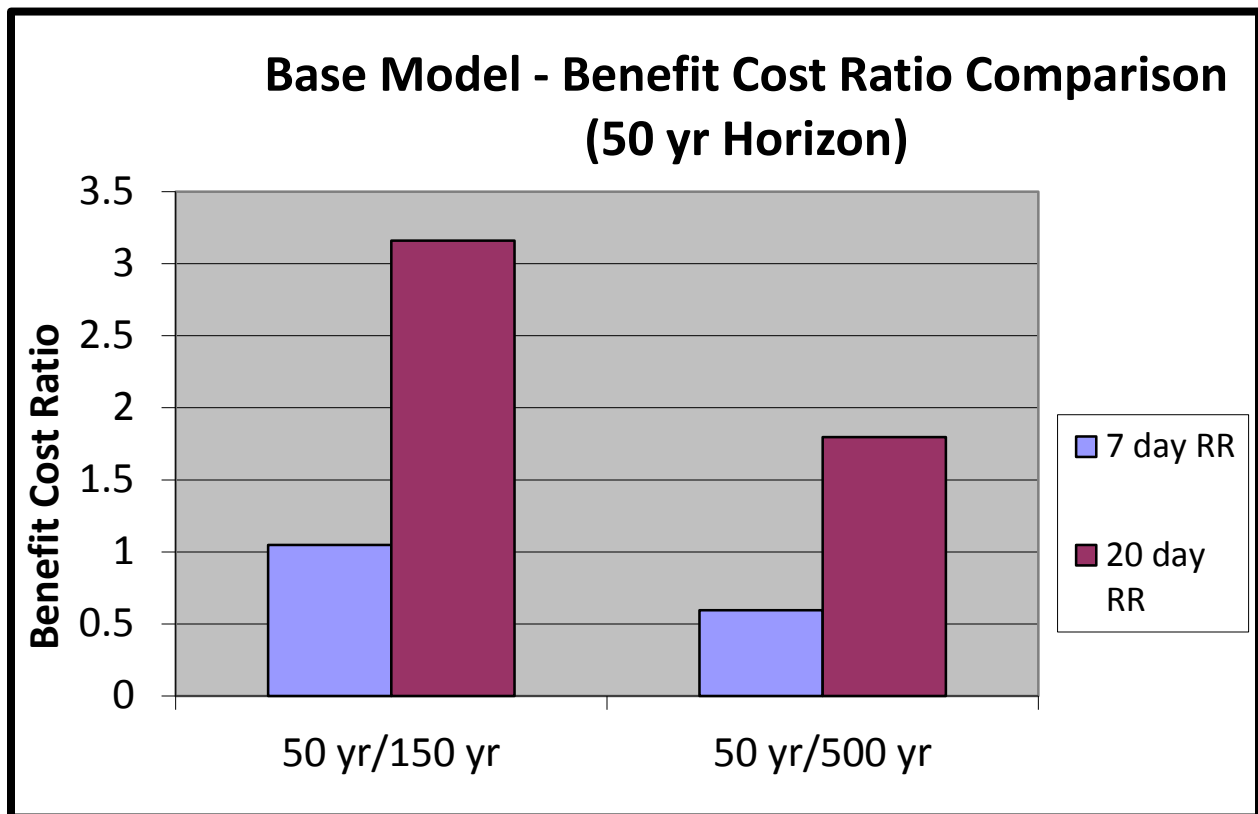


Figure 7.11 - Cost Benefit Ratio for Two Different Return Periods

8.0 Base Model with GT

In the revised model, gas turbine generators in 50 MW step sizes are added at the east bus point. The new line diagram is shown in Figure 8.1. A total number of 78 state contingencies are considered.

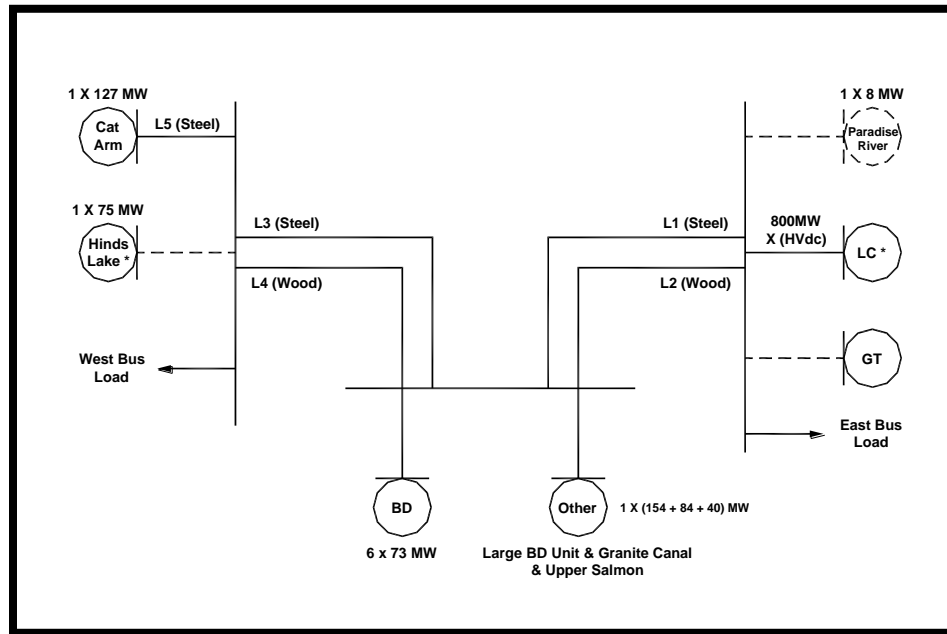


Figure 8.1 - Schematic Line Diagram with GT (East Bus)

8.1 Severity Index

Figure 8.2 presents the comparison of design options with one and two gas turbine units (50 MW and 100 MW) respectively. The base case analysis is done for a 50-year return period. The severity index is reduced almost by 50% if 100 MW is added for 2031 system loads. Figure 8.3 presents the information for a repair time of 20 days (severe line failure). Again, the severity index reduction is almost 40% if 100 MW of gas turbine is added for 2031 system loads.

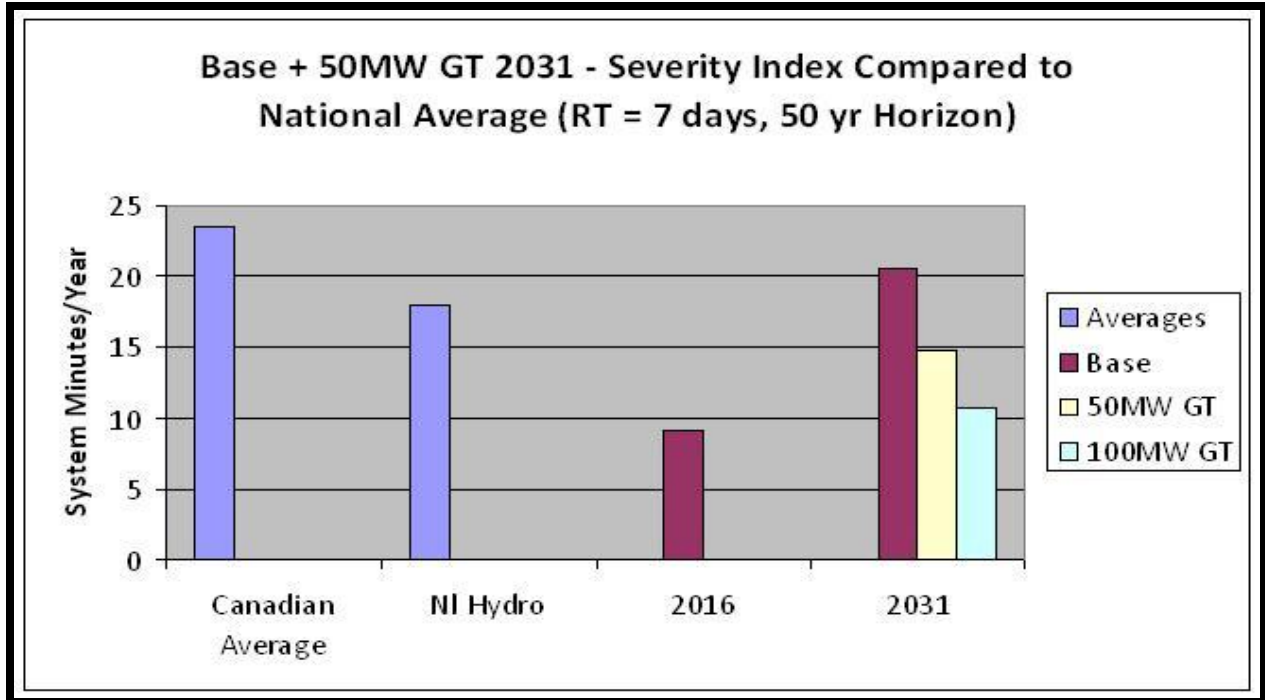


Figure 8.2 - Comparison of Severity Indices with GT added to the System (MTTR=7 days)

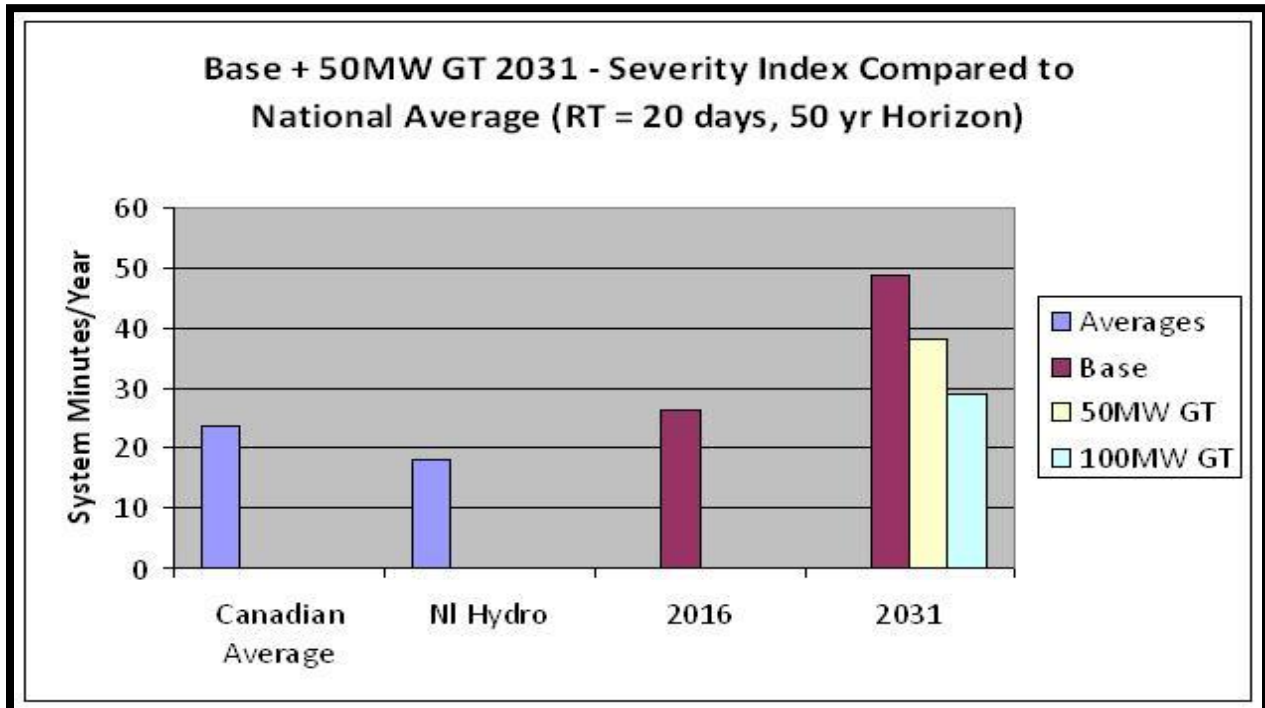


Figure 8.3 - Comparison of Severity Indices with GT Added to the System (MTTR=20 days)

8.2 ECOST

Figure 8.4 presents the **ECOST** versus two different planning horizon values. The **ECOST** for 50-year planning horizon is almost twice that of a 15-year planning horizon.

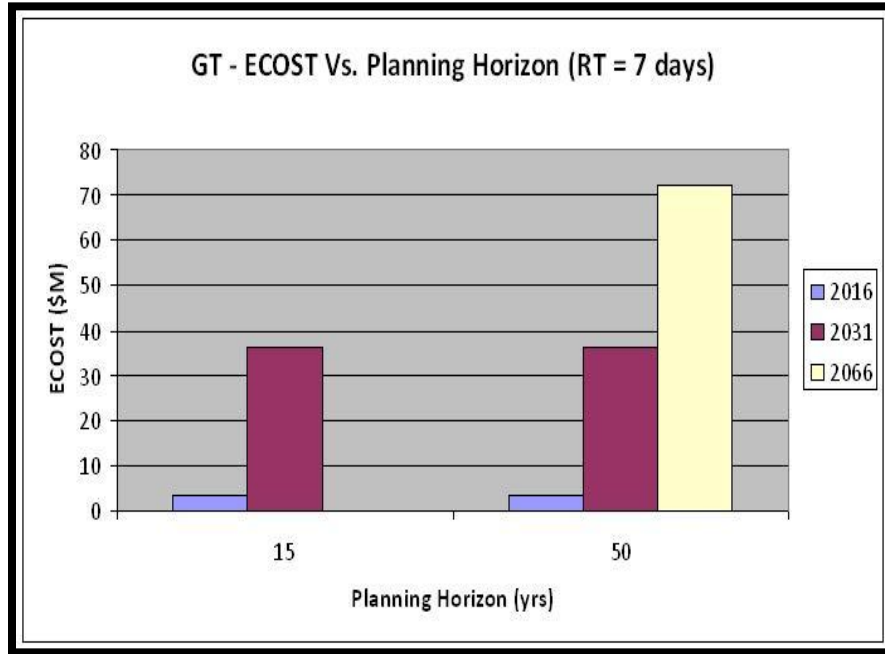


Figure 8.4 - Comparison of ECOST with GT for Two Planning Horizons

8.3 Benefit Cost Ratio (BCR)

Figure 8.5 presents the cost benefit analysis with GT added.

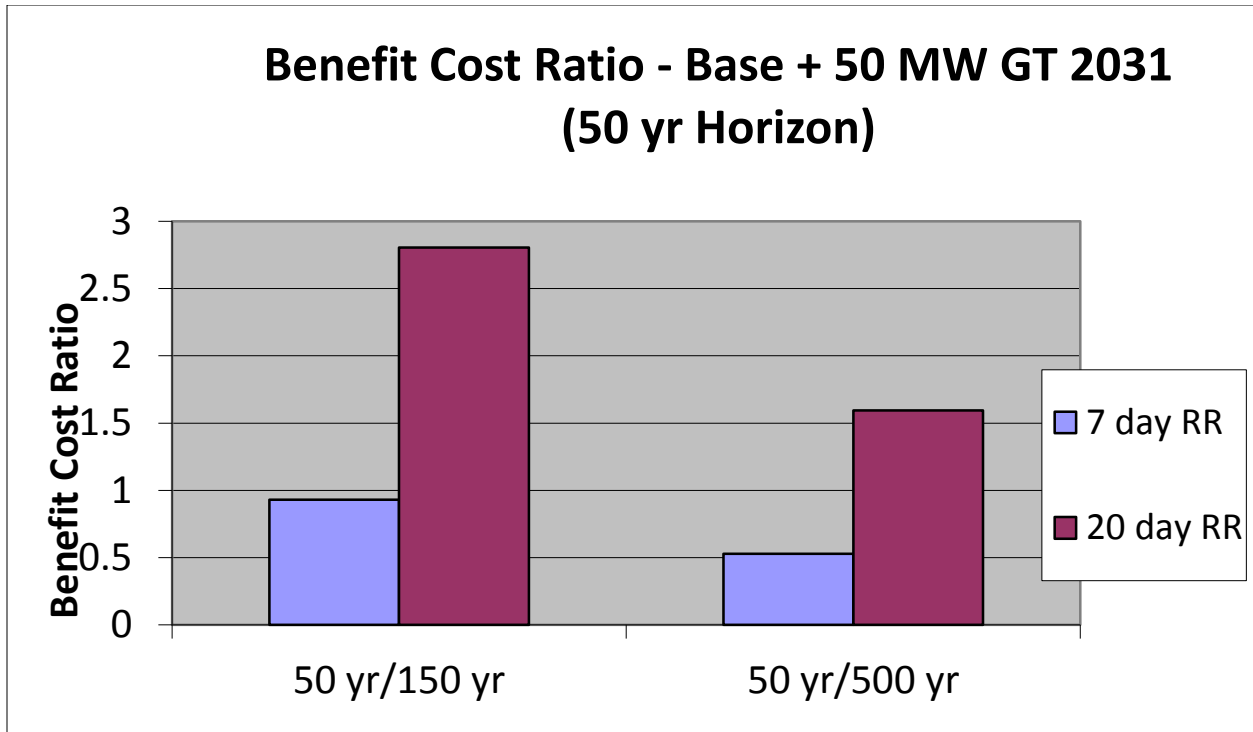


Figure 8.5 - Comparison of CBR for Two Different Return Periods

8.4 Comparative Assessment (Base Model and Base Model with GT)

Figure 8.6 presents the summary plot for all analyses with and without the GT. The data is for repair duration of 20 days. Each curve in Figure 8.6 represents a specific return period. The lower point on the curve is obtained from the base model while the three other points represent the total cost for base model supported with 50 MW, 100 MW and 150 MW of gas turbine respectively.

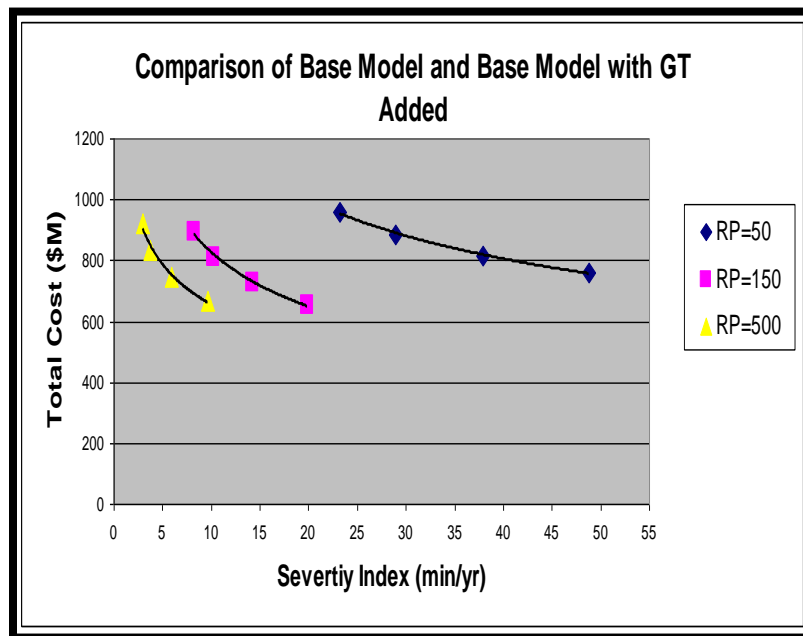


Figure 8.6 - Comparison of Base Model and Base Model with GT (RT=20 days)

Figure 8.7 presents the results for the base model and the base model with 50MW GT unit added. The severity index value for a 50-year return period line design with a 20-day repair duration is computed as 48 minutes per year based on the 2031 system load level (Figure 8.7). The corresponding total cost in 2016 dollars is \$759 million dollars. Since this SI value is considerably higher than the NLH outage value reported in the CEA study (Figure 4.13), an attempt was made to reduce this SI value by increasing GT

capacity in 50 MW step sizes. Table 8.1 presents the data for all return periods considering a 50 MW unit added to the base model (Figure 8.7).

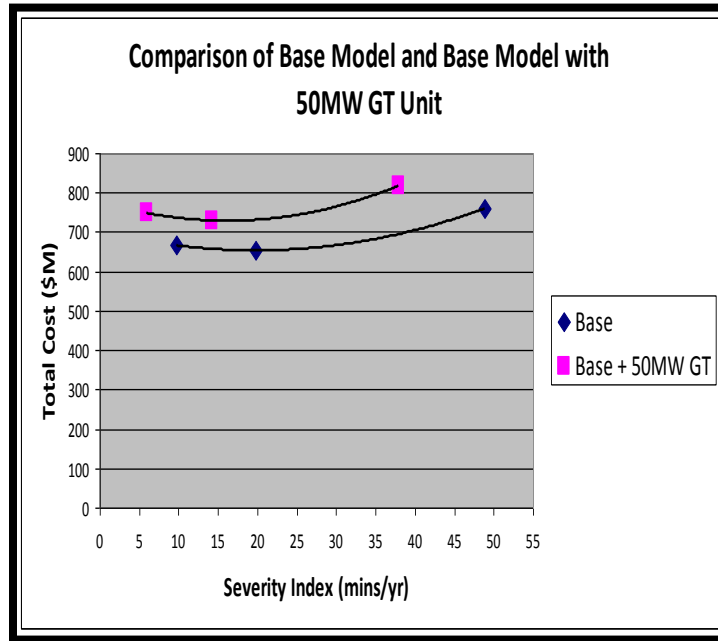


Figure 8.7 - Comparison of Base Model and Base Model with 50 MW GT (RT=20 days)

Table 8.1 – Comparative Assessment (Total Cost and Severity Index)

Return Period	Total Cost (10^6) – 2016 dollar(\$)			Severity Index (minutes/year)		
	50-year	150- year	500- year	50- year	150- year	500- year
BASE Model	759	653	666	48.81	19.84	9.69
BASE Model + 50MW GT intervened in 2031	817	729	748	37.90	14.24	5.95

It is noted that although the 50 MW gas turbine reduces the SI value by 30% for a 50-year design load, it is still considerably higher than the current NLH severity index value reported in the CEA study. Therefore, the alternative approach would be to consider a 150-year return period design with a 50 MW gas turbine added. This configuration will

reduce the severity index below the current NLH reported value. The total cost for this option will be \$729 million dollars (11% lower than its 50-year design option). According to Table 4.2, the degree of severity is classified as Level 2. Obviously to reduce the level further (i.e. to level 1), one needs to consider an option of 500-year return period with a 50 MW gas turbine added. This option will have a total cost of \$748 million dollars (16% higher than the base model cost with 150-year return period).

Based on this study, it appears that a 150-year return period with a 50 MW gas turbine unit added as back up generation will be the best option to consider. However, it is to be noted that the present study did not consider the submarine cable system and the converter stations in developing the system reliability model. Adding these two subsystems will increase the severity index further and may lead to the choice of a line design based on a higher return period (> 150 years) with additional generation support. This part has not been studied and should be considered seriously to achieve the best cost effective design of the HVdc line system.

9.0 Summary and Conclusions

The report presents a systematic methodology in determining the optimum design return period of a proposed \pm 450 kV HVdc line. The method uses the initial line cost which depends on the selected return period value chosen. For each return period value selected, a corresponding failure rate is determined and a number of repair days are assumed depending on the degree and extent of the HVdc line failure event.

A system model based on a probabilistic planning approach is developed to idealize the Hydro's existing 230 kV system identifying the HVdc line as a generation source. The adequacy indices are determined using an approximate "frequency and duration" computation methodology.

Based on the sensitivity analysis of various key parameters, it is shown that the optimum design return period will be 150-years if the HVdc line encounters a failure event that would require a 20-day repair duration to restore the line to service. However, if the line requires a seven day repair duration then the system severity index is reasonable and well below the Canadian national average as reported in the CEA study for a return period of 50-years.

To mitigate the large severity index value for a base model with a 50-year design return period and a 20 day repair duration, additional gas turbine support is considered for 2031 system loads (1 x 50 MW unit and 2 x 50 MW units). It is shown that the severity index values are reduced significantly if one uses 100 MW of gas turbine to support the existing system. The outage level is reduced by 38% for a 50-year design return period with line repair duration of 20 days.

The cost benefit ratio study in base model shows that the base model with design return periods of 150-years and 500-years can be justified compared to 50-year design considering the present value of the energy cost for a repair time of 20 days. In both cases the BCR is greater than 1.0.

However, considering both the severity index and the unsupplied energy cost, it appears that a design return period of 150-years with a 50 MW gas turbine unit added to the system will be the least cost option that will optimize the total line cost and also satisfy the system adequacy criteria (Table 4.2 and Figure 4.13).

It is to be noted that the present study did not consider the submarine cable system and the converter stations in developing the system reliability model. Adding these two subsystems will increase the severity index further and may lead to the choice of a line design based on a higher return period (> 150 years) with additional generation support. This part has not been studied and should be considered seriously to achieve the best cost effective design of the HVdc line system.

10.0 Recommendations

- Expand the study to include submarine cable system and the converters stations
- Include the submarine cable system and the converter stations in the system adequacy study to assess the severity indices and its impact on the optimum design return period of the line and costs
- Develop a database to construct customer damage function which reflects Nalcor energy service areas and customers
- Carry out an economic analysis study to assess the effects of the large capital investment which will be required to meet the load growth beyond 2031 and its impact on the optimum design return period.
- Expand the reliability study to include the Maritimes link and the power buy back option and its impact on the optimum return period and costs.
- Develop a plan for including probabilistic planning approach routinely in planning bulk electric power system

11.0 References

Billinton, Roy and Allan, Ron Reliability Evaluation of Power Systems, Plenum Press New York

Billinton, Roy and Allan, Ron Reliability Evaluation of Engineering Systems

Billinton Roy et. al 2001 Methods to consider Customer Interruption Costs in Power System analysis CIGRE Task Force Report No. 38.06.01, August, 100p.

Billinton, Roy. Wacker, G, and Wojczyuski, E. 1982. Customer Damage Relating from Electric Service Interruption, Canadian Electrical association R & D Project, 9007 U 131 report,

Billinton, Roy 2007 Contribution to CEATI project 3347 Transmission Line Failure Costs –Task Force Document under preparation (TF Leader Asim Haldar)

Billinton Roy and Zhang, Wei 1995 An Adequacy Equivalent Approach for Composite Power System Reliability Evaluation, Proceeding IEEE

Billinton Roy and Wangdee, Wijarn 2006 Bulk Electric System Reliability assessment, 6p

CEA Outage Report 2005 Forced Outage Performance of Transmission Equipment, Equipment Reliability Information system

CIGRE 2008 Technical Brochure on Big Storm Events, Lessons Learned

Endrenyi, J 1978 Reliability Modelling in electric Power Systems, Toronto, Wiley International

Ghajar, R.F. and Billinton, Roy 2006 Economic Cost of Power Interruptions: A Consistent Model and Methodology, Journal of Electric Power and Energy Systems, Volume 28, pp 29-35

Haldar, Asim 1995 Reliability Assessment of Transmission Line System on the Avalon Peninsula, Avalon Study Report

Haldar, Asim 2004 Reliability Based Management of Wood Pole Lines Technical Report Submitted to PUB, 20 year Asset Management Program for T& D department,

Haldar, Asim 2006 Upgrading of a 230kV Steel Transmission Line System Using Probabilistic Approach, Proceeding 9th International Conference on Probabilistic Methods Applied to Electric Power System (PMAPS), Stockholm, June 11-15, 7p

Li, Wenyuan Risk Assessment of Power Systems, Models, Methods and Application, **IEEE Press**, ISBN 0-471-63168-X © 2005

Peddle, Brent 2009 Engineering Work Term report on Software Development ECOST

Reddin Stephen 2008 Engineering Work Term Report on Software Development LCOST

Thomas, Peter 2009 Summary Letter Outlining the System Specification

Thomas Peter 2009 Private Discussion on Load beyond 2031 and generation gap

Tooktoshina, Brad 2009 Engineering Work Term Report on ECOST Model Development

Willette, Christopher 2008 Structural Analysis of HVdc Towers, Engineering Work Term Report

12.0 APPENDIX (Typical Input Data)

System Model				
Elements	Capacity (MW)	λ (/y)	No. of units	Remarks
BCE	73	0.3844	6	73 MW capacity comes from System Planning (A), λ (/y) is derived from 1998-2008 data from system operations (B)
Other	278	0.3844	1	Other is Granite Canal, Upper Salmon, Large BDE Combined. Capacity from System Planning (A), λ (/y) from same (B)
CAT ARM	127	0.3844	1	Cat Arm is two 63.5 MW units (A), although model as a single 127 MW unit. λ (/y) from (B)
Hind's Lake	75	-	1	Hind's Lake assumed to never fail and not connect to L5 (A), λ (/y) also from derived 1998-2008 hydraulic data (B)
X	800	-	1	HVdc line from Lower Churchill to the Avalon (East Bus)
L1	365	0.02	1	L1 is the rebuilt steel line from Bay D'Espoir to the Avalon (A)
L2	365	0.2	1	L2 is the wood pole line parallel to L1 from Bay D'Espoir to the Avalon (A)
L3	365	0.02	1	L3 is a tie line from Bay D'Espoir to the West bus (A)
L4	365	0.2	1	L4 is the second tie line from Bay D'Espoir to the West bus (A)
L5	365	0.02	1	L5 is the line connecting Cat Arm generation to the west bus (A)

Add on to east bus	Capacity (MW)	Total Generation
No Extra	0	1718

X - HVDC Line	50 Years	150 Years	500 Years
λ (/y)	0.02	0.006666667	0.002

μ (days)		
Hydraulic	HVdc	L1-L5
6.90	7	7.00

← μ (days) for hydraulic come from 1998-2008 data (B)

Peak Load	1508	← System Planning (C)
-----------	------	-----------------------

Load - Island (MW)	Weighted - East (MW)	Weighted - West (MW)	Percentage	Duration (h)
1365.02	928.60	436.42	3%	262.8
1178.83	801.94	376.89	17%	1489.2
942.52	641.18	301.34	30%	2628
799.54	516.70	242.84	20%	1752
606.41	412.53	193.88	30%	2628

CDF (\$/KW)	Interruption Duration (hours)				
	0.016666667	0.333333333	1	4	8
Industrial	2.702095417	6.432722813	15.10898232	41.8461226	92.80243504
Residential	0.633303613	4.937422615	14.22235726	52.0610127	138.0425959
Commercial	0.001172784	0.15480755	0.801011792	8.17196218	26.09210887
TOTAL	3.396571815	11.52495298	30.13235136	102.099098	256.9371398

Load - West Percentage	0.319715349
Load - East Percentage	0.680284651

Sector Distribution

Load (%)	Sector Energy (%)
Industrial	0.0869
Residential	0.6301
Commercial	0.2831